

ISSN 0030-6096

OSAKA CITY MEDICAL JOURNAL



2021

PUBLISHED BY
OSAKA CITY MEDICAL ASSOCIATION
OSAKA JAPAN

Osaka City Medical Journal
Vol. 67, No. 2, December 2021

CONTENTS

	page
High Calorie Diet, Low Body Weight and Hypothermia Limit Body Weight Gain in Hospital Treatment for Anorexia Nervosa-restricting Type KAZUYA NISHIMOTO, TSUNEO YAMAUCHI, TOMOKO HARADA, SAORI MIYAMOTO, MIHOKO HONDA, TAKUMI MATSUZUKA, and KOKI INOUE	57
Primarily Outcome Report of Our Updated Structural Strategy for Treating Patients with Acute Respiratory Distress Syndrome Following Corona Virus Disease 2019 during the Third Pandemic Phase in Japan KENICHIRO UCHIDA, KENJI MATSUO, SAE KAWATA, AYAKO KIRITOSHI, RYO DEGUCHI, HOSHI HIMURA, MASAHIRO MIYASHITA, KATSUMI YAMAMOTO, SHINICHIRO KAGA, TOMOHIRO NODA, TETSURO NISHIMURA, HIROMASA YAMAMOTO, and YASUMITSU MIZOBATA	69
An Analysis of Compensatory Trunk Movements in Shoulder Joint Movements: Application to Healthy Individuals and Patients after Shoulder Joint Surgery TAMOTSU NAKATSUCHI, MITSUHIKO IKEBUCHI, TAKAHIRO NISHINOHARA, SHIGEYOSHI NAKAJIMA, and HIROAKI NAKAMURA	81
—Case Report—	
Orbital Venous Malformation with Obscure Clinical Symptoms Diagnosed by Contrast-enhanced Magnetic Resonance Imaging in a Different Body Position AKIKA KYO, YUSAKU YOSHIDA, MIZUKI TAGAMI, MASAO HAMURO, and SHIGERU HONDA	91

High Calorie Diet, Low Body Weight and Hypothermia Limit Body Weight Gain in Hospital Treatment for Anorexia Nervosa-restricting Type

KAZUYA NISHIMOTO, TSUNEO YAMAUCHI, TOMOKO HARADA, SAORI MIYAMOTO,
MIHOKO HONDA, TAKUMI MATSUZUKA, and KOKI INOUE

Department of Neuropsychiatry, Osaka City University Graduate School of Medicine

Abstract

Background

There are considerable individual differences in how body weight increases in response to calorie intake in hospitalized patients with anorexia nervosa (AN); however, the extent of the factors influencing weight gain remain unclear. Thus, this study aimed to clarify the relationship between body mass index (BMI) gain in hospitalized female AN patients and factors including calorie intake, body weight, and body temperature.

Methods

Subjects were 56 female anorexia nervosa-restricting type (AN-R) patients who had been hospitalized for at least 60 days. Age, height, body weight, body temperature, blood test results, and calorie intake were surveyed. BMI gain was defined as the difference when predicted BMI calculated using calorie intake beginning on day 30 of hospitalization was subtracted from actual BMI on day 60. The effects of calorie intake, body weight, body temperature, presence of liver dysfunction, age, and disease duration were explored using multiple regression analysis.

Results

With regard to BMI gain, the higher total calorie intake, lower weight on day 30, and lower mean body temperature during the latter period of hospitalization were, weight gain was found to fall significantly below the expected level. Relationships were not found with presence of liver dysfunction, age, and disease duration.

Conclusions

It is likely that weight did not increase as much as expected from calorie intake in AN patients with severe low body weight due to physical abnormalities. We must consider the extent of their recovery from critical physical issues.

Key Words: Weight gain; Anorexia nervosa-restricting type; Body mass index; Calorie intake; Hypothermia

Received September 4, 2020; accepted January 12, 2021.

Correspondence to: Kazuya Nishimoto, MD.

Department of Neuropsychiatry, Osaka City University Graduate School of Medicine,
1-4-3 Asahimachi, Abeno-ku, Osaka 545-8585, Japan

Tel: +81-6-6645-3821; Fax: +81-6-6636-0439

E-mail: k.nishimoto.1985@gmail.com

Introduction

Anorexia nervosa (AN) is an eating disorder (ED) with a high mortality rate resulting from severe low body weight caused by refusal of food¹⁻⁴⁾. While eating disorders are primarily treated on an outpatient basis, inpatient treatment is recommended for patients in critical physical condition due to their low body weight⁵⁻⁷⁾. The goal of hospital treatment is to manage physical condition while increasing body weight by returning to an appropriate intake of nutrients. Weight at discharge is an important prognostic factor for long-term prognosis with higher weight shown to lead to a better prognosis⁸⁻¹⁰⁾. Meanwhile, low body weight at the time of admission is also linked to extended hospitalization¹¹⁾. However, it is best to avoid extended hospital stays because of the mental stress on patients and financial reasons. Thus, effective weight gain during hospitalization is essential. In recent years, rapid refeeding for the purpose of efficient weight gain has become the standard treatment, and eventually patients may consume nearly 3000 kcal/day^{12,13)}.

Hospitalized AN patients show individual differences in the speed and level of weight gain depending primarily on calorie intake¹²⁻¹⁵⁾. However, clinically, weight gain can be smaller or even larger than the amount expected based on calorie intake. It is unclear whether this variance takes place as a result of differences in the physical condition of individual patients, or due to resistance to treatment that has gone unnoticed by medical workers such as excessive activity, discarding of food, or self-induced vomiting, which are commonly seen during hospitalization. Clinicians may sometimes suspect that these disappointing results are due to a lack of motivation for treatment or resistance on the part of the patient, thereby unfortunately worsening the relationship between doctor and patient. Nonetheless, there remains insufficient research clarifying factors related to weight gain during hospitalization.

Metabolic amount, which is influenced by a multitude of factors, is generally considered to have a major involvement in weight gain. In AN patients, a condition in which patients have severely low body weight, basal metabolic rate (BMR) is low¹⁶⁻¹⁸⁾. Additionally, aging is also associated with progressive declines in BMR^{19,20)}. Further, the endocrine system has a major impact on metabolism, and endocrine abnormalities are common in chronic AN patients²¹⁻²⁴⁾. Body temperature has a reciprocal relationship with metabolism²⁵⁾, and it is no surprise that most AN patients are hypothermic^{7,26,27)}. Body temperature are reversible and can all be improved in AN patients by returning to proper nutrition through treatment^{26,28)}.

Organ dysfunction is another factor involved in weight gain. Liver dysfunction in particular is a form of organ dysfunction characteristic to low body weight AN^{6,7,29,30)}. In this context, research has shown that the amount of weight gain after admission is lower than normal in AN patients with liver dysfunction³⁰⁾. AN patients are also known to frequently exhibit digestive dysfunction³¹⁻³⁴⁾. Further, it is likely that, as the duration of AN increases, organ dysfunction and physical complications will become more serious⁷⁾.

In clinical settings, it is not uncommon to see sudden and drastic increases or decreases in weight at the start of hospitalization due to dehydration or edema present at admission^{14,35-38)}. Yet, most past research on weight gain during hospitalization have used body weight and body mass index (BMI) measurements taken on the day of admission^{11-15,30,35-40)}. This leads to several problems. For example, the lower body weight is on the day of admission, the higher the rate of increase in body weight and BMI will be thereafter¹¹⁾. However, these studies did not consider that weight gain changes over time in accordance with individual calorie intake levels.

In the present study, we decided the starting day as the one at which the irregular body weight fluctuations found at the start of hospitalization had largely disappeared and considered BMI gain thereafter by subtracting the predicted BMI estimated using calorie intake from the actual BMI measured on day 60 of hospitalization. Subjects were patients with anorexia nervosa-restricting type (AN-R). Because these patients do not binge-eating and purging, their body weight fluctuations at the start of hospitalization are lesser than those in patients with AN binge-eating/purging type (AN-BP)³⁷⁾. This study aimed to clarify the relationship between BMI gain and factors hypothesized to influence it, namely, calorie intake, body weight, body temperature, presence of liver dysfunction, age at admission, and disease duration.

Methods

Patients

This was a retrospective cohort study based on the medical records of eating disorder patients admitted to the neuropsychiatry ward at Osaka City University Hospital between April 1, 2012 and March 31, 2018. There were 143 patients satisfying the Diagnostic and Statistical Manual of Mental Disorders, 5th ed. (DSM-5)⁴¹⁾ diagnostic criteria for AN, of which 87 (60.8%) were classified as AN-R, and 56 (39.2%) were classified as AN-BP. Of those with AN-R, 29 patients (33.3%) with a hospitalization period of under 60 days and 2 patients (2.3%) who were male were excluded for an end total of 56 subjects (64.4%).

Procedure

Age at admission, disease duration, height at admission, body weight, body temperature, blood test data, and daily calorie intake from the day of admission to day 60 of hospitalization were extracted from subjects' medical records. Body weight was measured and recorded every 1-7 days according to the patient's physical condition. Axillary body temperature, which was taken every morning, was averaged for every 10 days after hospitalization. Patients with maximum values of AST or ALT recorded as being above grade 3 (either AST >175 U/L or ALT >150 U/L), based on the Common Terminology Criteria for Adverse Events (CTCAE) version 5.0⁴²⁾ standards, during the 60 days of hospitalization were classified as having liver dysfunction. The daily calorie intake is based on medical records. The amount of carbohydrates, proteins, and fats in each meal was measured by the dietitian, and calories were calculated using the modified Atwater system (4 kcal/g for carbohydrates and proteins, 9 kcal/g for lipids)⁴³⁾. Patients were required to consume all of the food provided, and the percentage of consumption was recorded. Calories for nasogastric tube feeding and intravenous drip were added to the calorie intake, if performed.

Measures

Day 30 of hospitalization was used as the starting day for comparison, when body weight gain was judged to have stabilized. BMI gain was defined as the BMI (kg/m²) difference obtained when predicted BMI calculated using calorie intake was subtracted from actual BMI on day 60 of hospitalization. Estimated body weight was calculated by adding the expected amount of weight gain (calculated from total calorie intake during that period) from the initial day to the next day that body weight was measured. When calculating expected weight gain, every 7000 kcal remaining after subtracting the patient's total energy expenditure from the total calorie intake was established as corresponding to 1 kg of body weight^{43,44)}. Total energy expenditure was calculated by multiplying BMR and activity factors. There is no ideal formula for calculating BMR for low body weight AN. In

this study, we adopted the Ganpule equation [BMR (kcal)={0.0481×body weight (kg)+0.0234×height (cm)−0.0138×age (years)−0.9708}×1000/4.186], which includes the basic parameters that constitute most formula for BMR⁴⁵⁾. Activity factors were determined by the extent of activity while hospitalized (confined to bed 1.2, out of bed 1.3)⁴⁶⁾. The extent of activity was always strictly controlled in the closed ward. Patients with extremely low body weight were confined to bed, and out of bed activities were permitted according to the degree of weight gain.

Statistics

Mean body temperature, BMI, and body weight after admission were analyzed using repeated measures ANOVA and the Bonferroni post hoc test. To determine the validity of the starting day, when weight gain after hospitalization was thought to have stabilized, the error between BMI derived using the connection between BMI at admission and BMI on day 60 of hospitalization and actual BMI was analyzed using a chi-squared test. Factors impacting BMI gain were explored using multiple regression analysis. Concerning independent variables, age at admission was entered using the force entry method, while total calorie intake, weight on day 30 of hospitalization, mean body temperature over days 1-10 of hospitalization, mean body temperature over days 51-60 of hospitalization, presence of liver dysfunction, and disease duration were entered using the stepwise method. A two-tailed p value of less than 0.05 was considered significant. Data were analyzed using SPSS26.0 for Mac OS X (SPSS Japan, Tokyo, Japan). Due to the retrospective nature of this study, personal data were protected and individuals were not identified; informed consent could not be obtained. The research protocol was reviewed and approved by the Ethics Committee of Osaka City University.

Results

Subjects' mean age at admission was 18.04±7.73 years. Grouping by age reveals that most participants were young, with 18 patients under the age of 15 (32.1%), 26 between the ages of 15 and 19 (46.4%), 6 between the ages of 20 and 24 (10.7%), 2 between the ages of 25 and 29 (3.6%), and 4 aged 30 or above (7.1%). Mean BMI at admission was 11.73±1.60, and 55 subjects (98.2%) had a BMI below 15, which is classified as most severe in the DSM-5 diagnostic criteria. The disease duration from onset to admission was less than 1 year for 17 subjects (30.0%) and less than 3 years for 45 subjects (80.0%), but was over 20 years for 2 subjects (3.6%). Mean body weight at admission was 27.73±4.80 kg. This was on mean 13.89±7.22 kg lower than their weight before the onset of EDs, and body weight had dropped by over 10 kg for 36 patients (62.3%). During the 60 days of hospitalization, mean maximum values of AST was 112.13±371.25 U/L, and mean maximum values of ALT was 152.45±326.23 U/L. Fourteen patients had liver dysfunction. Of these, 5 satisfied the criteria for both AST and ALT, 9 for ALT alone, and none for AST alone. Mean total calorie intake during the 60 days of hospitalization was 108.21±23.21 Mcal (protein 18.10±4.62 Mcal; fat 24.02±6.87 Mcal; carbohydrates 66.10±13.61 Mcal). Mean total calorie intake from day 30 to 60 was 65.43±13.30 Mcal (protein 10.17±2.64 Mcal; fat 14.01±4.37 Mcal; carbohydrates 40.42±10.43 Mcal). (Table 1)

Table 2 shows body weight and BMI every 10 days, and mean body temperature for each 10-day period after admission. With respect to mean body weight and BMI, comparison between measures at admission and on day 60 of hospitalization revealed that both increased significantly by 4.86 kg in weight and 2.06 kg/m² in BMI, respectively. There were substantial individual differences in weight and BMI gained by each subject over the 60-day hospitalization period with body weight changes

Table 1. Clinical characteristics

	Toal (N=56)
Age (years) ^a	18.04±7.73
Height (cm) ^a	153.60 (150.58, 157.03)
Body weight (kg) ^a	27.73±4.76
BMI (kg/m ²) ^a	11.73±1.59
Disease duration (years) ^b	1.50 (0.92, 2.43)
Age of onset of EDs (years)	15.02±3.93
Weight before the onset (kg/m ²)	41.63±8.92
Liver dysfunction ^c	14/56 (25)
Total calorie intake (Mcal) ^c	108.21±23.20

Date are means±SD, median (25 percentile, 75 percentile), or n (%). Patients with maximum values of AST or ALT recorded either AST >175 U/L or ALT >150 U/L were classified as having liver dysfunction.

^a at admission. ^b from onset to admission. ^c during the 60 days of hospitalization. BMI, body mass index; and ED, eating disorder.

Table 2-1. Body weight and BMI every 10 days after admission

	Day 1	Day 10	Day 20	Day 30	Day 40	Day 50	Day 60
Body weight (kg)							
Mean ^{*a}	27.73	28.90	29.29	30.00	30.98	31.95	32.59
(SD)	4.76	5.15	5.01	5.07	5.14	5.28	5.37
BMI (kg/m ²)							
Mean ^{*a}	11.73	12.21	12.39	12.69	13.11	13.52	13.79
(SD)	1.59	1.77	1.73	1.77	1.79	1.84	1.86

Table 2-2. Mean body temperature for each 10-day period after admission

	Days 1-10	Days 11-20	Days 21-30	Days 31-40	Days 41-50	Days 51-60
Mean body temperature (°C)						
Mean ^{*b}		36.48	36.64	36.68	36.67	36.72
(SD)		0.35	0.28	0.27	0.23	0.29

n=56, *p<0.05. (Statistically significant)

^a Body weight and BMI increased significantly every 10 days after admission, except between day 10 and day 20.

^b Mean body temperature over days 1-10 of hospitalization was significantly lower than other periods. BMI, body mass index.

ranging from -0.90 kg to +10.00 kg and BMI changes ranging from -0.39 kg/m² to +4.44 kg/m². While some patients did show sudden and drastic weight gain or loss at the start of hospitalization, only one patient lost weight between day 30 and day 60 of hospitalization. In order to select a starting date at which the irregular fluctuations in body weight at the start of hospitalization had abated and BMI gain had stabilized, we calculated the chi-squared value for the error between actual BMI and BMI derived using the connection between BMI at admission and BMI on day 60 of hospitalization. The chi-squared value increased from admission onward, peaking at 5.35 on day 12 before decreasing continuously until day 60. Values were 4.07 on day 10, 1.22 on day 20, and 0.65 on day 30. The error

had largely disappeared on day 30. Thus, day 30 was decided as the starting day. Body temperature fluctuated greatly day to day and was therefore represented with an average every 10 days. Mean body temperature over days 51-60 during the latter period of hospitalization increased significantly to $36.69 \pm 0.27^\circ\text{C}$ compared to $36.48 \pm 0.35^\circ\text{C}$ over days 1-10 during the early period of hospitalization.

The relationships between total calorie intake and BMI gain were illustrated as scatter plots in Figure 1. The relationships between mean body temperature and BMI gain were illustrated as scatter plots in Figure 2. The relationships between body weight on day 30 of hospitalization and BMI gain were illustrated as scatter plots in Figure 3. As these scatterplots demonstrate linear relationships, a multiple regression analysis was performed.

Table 3 shows the results of multiple regression analysis using the force entry and stepwise methods for factors impacting BMI gain. Although a significant relationship was not found for age at admission ($\beta=0.16$, $p=0.11$), significant relationships were found for total calorie intake ($\beta=-0.74$, $p<0.01$), body weight on day 30 of hospitalization ($\beta=0.27$, $p<0.05$), and mean body temperature over days 51-60 of hospitalization ($\beta=0.43$, $p<0.01$). In the final model, the normality of the residuals were analyzed using the Shapiro-Wilk test and confirmed as $p=0.764$. All VIFs were less than 10.0, so there were no multicollinearities. The Durbin-Watson ratio was 1.724 and there were no outliers.

This study concludes that a higher total caloric intake was associated with a lower BMI gain compared to the predicted gain, while a higher mean body temperature during the latter period of hospitalization and a higher starting weight were associated with a higher BMI gain. However, mean body temperature over days 1-10, presence of liver dysfunction, age at admission, and disease duration were not found to be significantly associated with BMI gain.

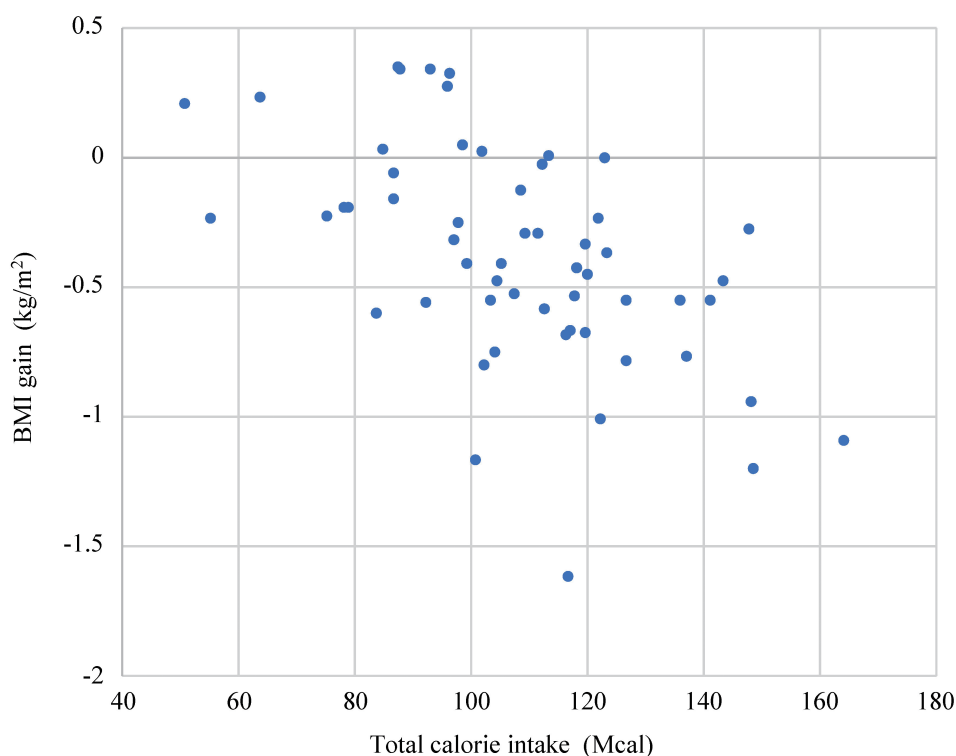


Figure 1. The relationship between total calorie intake and body mass index (BMI) gain.

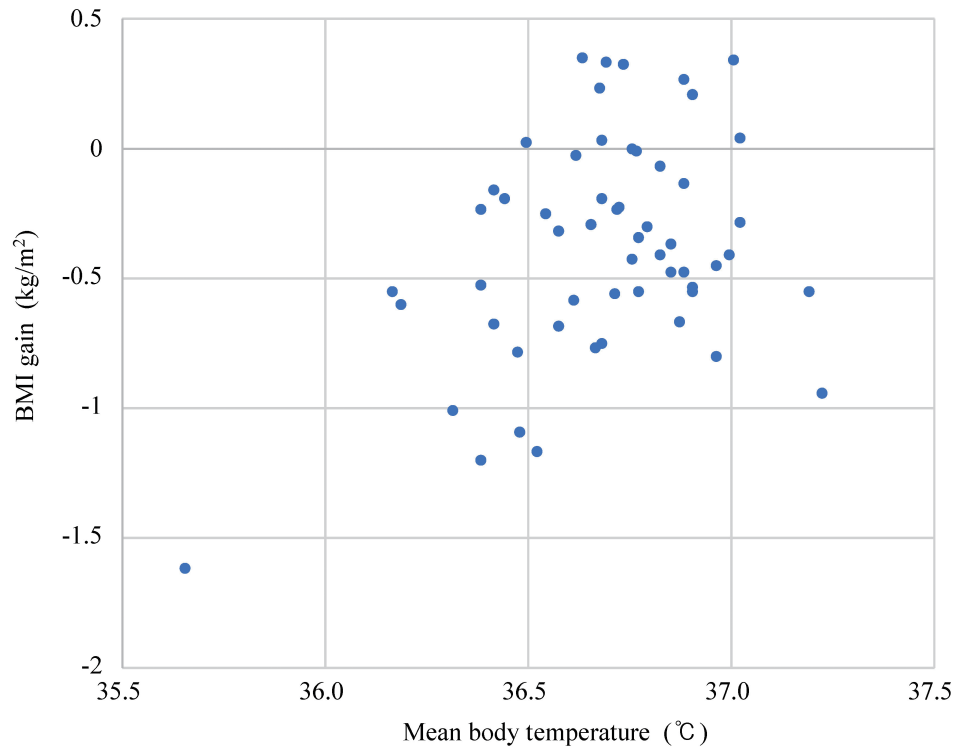


Figure 2. The relationship between mean body temperature over days 51-60 and body mass index (BMI) gain.

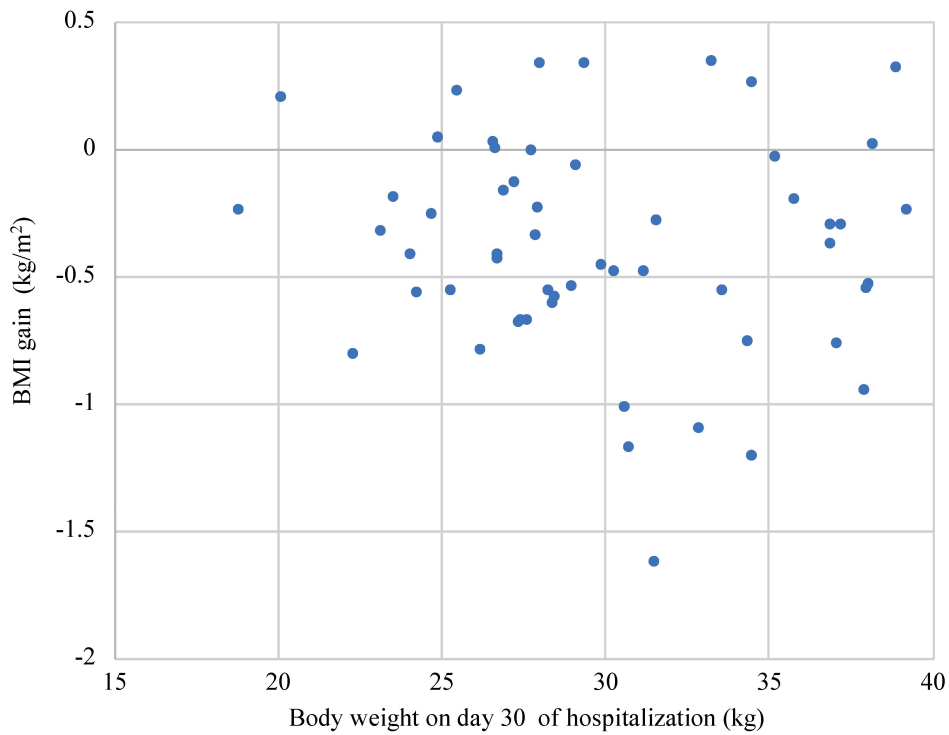


Figure 3. The relationship between body weight on day 30 of hospitalization and body mass index (BMI) gain.

Table 3. The results of multiple regression analysis using the force entry and stepwise methods for factors impacting BMI gain

	B	95% confidence interval for B		R ²	Adjusted R ²	F
		β	Lower limit			
Age at admission (years)	0.01	0.16	-0.002	0.02		
Total calorie intake (Mcal) ^a	-0.013	-0.74*	-0.017	-0.009		
Mean body temperature over days 51-60 of hospitalization (°C)	0.67	0.43*	0.37	0.97		
Body weight on day 30 of hospitalization (kg)	0.02	0.27*	0.004	0.04		
					0.54	0.51
						15.11*

Concerning independent variables, age at admission was entered using the force entry method, while total calorie intake, weight on day 30 of hospitalization, mean body temperature over days 1-10 of hospitalization, mean body temperature over days 51-60 of hospitalization, the presence of liver dysfunction, and disease duration were entered using the stepwise method. The final model accounted for 51% (F=15.11, p<0.01) of the variance.

n=56, *p<0.05. (Statistically significant) ^aduring the 60 days of hospitalization. B, unstandardized coefficient; β , standardized partial regression coefficient; and BMI, body mass index.

Discussion

This study aimed to clarify the relationship between BMI gain and calorie intake, body weight, body temperature, presence of liver dysfunction, age at admission, and disease duration in hospitalized patients with AN-R. As a result, BMI gain was found to be significantly lower than the predicted amount when total calorie intake during hospitalization was higher, weight on day 30 of hospitalization was lower, and mean body temperature over days 51-60 during the latter period of hospitalization was lower. Meanwhile, presence of liver dysfunction, age at admission, and disease duration were not shown to have a significant relationship with BMI gain.

Generally, it can be assumed that consuming more food will lead to more weight gain. High calorie diet on admission was reported to be associated with rapid recovery^{12,15}. In this study, AN patients consumed enough food to have a calorie surplus, and indeed, most patients gained weight over the hospitalization period. However, BMI gain was found to fall below the level expected when total calorie count was higher.

It is worth noting that impaired digestion and absorption of nutrients in AN patients may have impacted this result. In this context, research using eating disorder model mice demonstrated that increased colonic permeability and histological alterations—caused by the eating disorder—result in impaired absorption of nutrients⁴⁷. These findings suggest that a similar change also occurs in human AN patients. Moreover, food spending a longer period of time in the stomach due to weakening of the gastrointestinal tract and reduced digestive function caused by issues such as constipation are inevitable complications in clinical AN patients³²⁻³⁴. In this study as well, the amount of food provided during hospitalization likely surpassed the capacity for digestion and absorption of AN patients, who have a poorer ability to digest and absorb nutrients than healthy individuals.

Meanwhile, reduction in the amount of energy necessary to maintain functioning will increase the calorie surplus, which makes it easier to gain weight. This is largely influenced by BMR which, as demonstrated by the Ganpule equation, increases with body weight⁴⁵. In the past, some studies used indirect calorimetry to measure basal metabolism^{17,18,21,28}. However, the method of estimating the

predicted body weight and comparing with the measured body weight as in this study has not been used in previous studies. In this study, basal metabolism increases with weight gain over the course of treatment as in previous studies. However, this is contrary to our finding that higher body weight increased the likelihood of weight gain. In the body composition of AN patients, FM is extremely low, meaning that the ratio of FFM is high relative to that of healthy individuals³⁷). When AN patients rapidly gain weight over a short period by increasing food intake, the formation of tissues with a high BMR, like muscle¹⁶⁻¹⁸), is likely to be limited by the hospital environment in which patients do not exercise. Thus, the BMR for AN patients in the process of recovery with a relatively high body weight may have been lower than the BMR calculated from their actual body weight in this study. On the other hand, past studies have found that AN patients preferentially recovered FFM, and that FFM requires less energy than FM to be increased⁴⁸). Thus, future research would benefit from measuring the FM and FFM comprising subjects' body compositions.

Body temperature is thought to be an indicator indirectly reflecting BMR²⁵). Moreover, AN patients are known to often become hypothermic^{7,26,27}). In clinical settings, patients often temporarily experience drastic fluctuations in body temperature, particularly at the start of hospitalization, due to the impact of factors such as circulatory dynamics and dehydration accompanying changes in their diet and living environment⁴⁹). Increase in body temperature during hospitalization represents an increase in BMR and was hypothesized to inhibit weight gain, but our results showed that the opposite is true. Although there has been minimal research on body temperature changes in AN, Belizer CM et al suggested that recovery from hypothermia in AN may be a predictor of physical recovery²⁶). In the present study, mean body temperature increased significantly over time from the early period of hospitalization. Thus, high body temperature during the latter period of hospitalization may have represented physical improvements including recovery from impaired digestion, absorption, and organ dysfunction.

The various organ dysfunctions that often complicate AN have been shown to accelerate metabolism^{46,50,51}) and may reduce excess calories used for weight gain. Liver dysfunction is seen at a particularly high frequency in AN^{30,31}). Additionally, it has been reported to make weight gain more difficult than normal³⁰). The extent of organ dysfunction is incorporated into the equation for calculating basal metabolism as stress factors^{46,50,51}). However, there is no clear consensus regarding stress factors. For example, some findings to the contrary indicate that there is only one or less stress factors in a state of chronic malnutrition⁵⁰). In the present study, when calculations were performed with stress factors of 1, presence of liver dysfunction was not found to have a significant relationship with BMI gain, and thus, presence of liver dysfunction was not found to impact basal metabolism. In determining the stress factors, it is essential to consider the complex relationships between various factors including organ dysfunction, particularly liver dysfunction.

Although BMR decreases with aging^{19,20}), age at admission was not significantly associated with BMI gain in the present study. Past studies exploring age and disease duration have also been unable to identify significant associations^{38,39,52}). The fact that most participants were in their 20s or younger and had a disease duration of less than three years may partially explain why a significant relationship was not found.

The present study has several limitations. Because there is no formula for calculating basal metabolism indicated for extremely low body weight AN, the Ganpule equation validated in patients with BMI 16.5 to 36.4 kg/m² was utilized. However, the mean BMI of the patients in this study was

lower, so its suitability may be drawn into question. Additionally, it would have been necessary to measure gastrointestinal symptoms such as diarrhea in order to clarify the presence of malabsorption. It also would have been optimal to carry out measurements and tests evaluating body temperature and liver dysfunction with more meticulous methods and timings. Further, there were only 56 subjects. Analysis of a larger sample may have shown relationships not detected in the present study. Moreover, AN patients resistant to weight gain are often observed resisting treatment by methods such as discarding food or vomiting while under hospital care. Although subjects' behaviors were carefully monitored during the hospitalization period, the possibility that some subjects did not consume all the food provided cannot be completely ruled out.

In conclusion, this study found that individual physical factors may impact BMI gain during hospitalization in AN-R patients. Therefore, we must consider the extent of their recovery from critical physical issues. The results of the present study are valuable in that they encourage clinicians to avoid suspecting patients of behaviors deviating from their treatment plan when weight gain does not match calorie intake in the inpatient treatment of AN. Thus, it is hoped that future research can shed further light on the factors involved in weight gain and their impact.

Acknowledgments

All authors have no COI to declare regarding the present study.

References

1. Arcelus J, Mitchell AJ, Wales J, et al. Mortality rates in patients with anorexia nervosa and other eating disorders. A meta-analysis of 36 studies. *Arch Gen Psychiatry* 2011;68:724-731.
2. Mitchell JE, Crow S. Medical complications of anorexia nervosa and bulimia nervosa. *Curr Opin Psychiatr* 2006;19:438-443.
3. Hoang U, Goldacre M, James A. Mortality following hospital discharge with a diagnosis of eating disorder: national record linkage study, England, 2001-2009. *Int J Eat Disord* 2014;47:507-515.
4. Nielsen S, Møller-Madsen S, Isager T, et al. Standardized mortality in eating disorders: a quantitative summary of previously published and new evidence. *J Psychosom Res* 1998;44:413-434.
5. National Collaborating Centre for Mental Health (UK). Eating disorders: Core interventions in the treatment and management of anorexia nervosa, bulimia nervosa and related eating disorders. Leicester UK: The British Psychological Society & The Royal College of Psychiatrists; 2004.
6. Working Group, Royal College of Psychiatrists. Guidelines for the nutritional management of anorexia nervosa. London: Royal College of Psychiatrists; 2005 July. Council Report CR130.
7. Hay P, Chinn D, Forbes D, et al. Royal Australian and New Zealand College of Psychiatrists clinical practice guidelines for the treatment of eating disorders. *Aust N Z J Psychiatry* 2014;48:977-1008.
8. Bean P, Loomis CC, Timmel P, et al. Outcome variables for anorexic males and females one year after discharge from residential treatment. *J Addict Dis* 2004;23:83-94.
9. Baran SA, Weltzin TE, Kaye WH. Low discharge weight and outcome in anorexia nervosa. *Am J Psychiatry* 1995;152:1070-1072.
10. Lock J, Litt I. What predicts maintenance of weight for adolescents medically hospitalized for anorexia nervosa? *Eat Disord* 2003;11:1-7.
11. Hart S, Abraham S, Franklin R, et al. Weight changes during inpatient refeeding of underweight eating disorder patients. *Eur Eat Disord Rev* 2011;19:390-397.
12. Madden S, Miskovic-Wheatley J, Clarke S, et al. Outcomes of a rapid refeeding protocol in Adolescent Anorexia Nervosa. *J Eat Disord* 2015;3:8.
13. Peebles R, Lesser A, Park CC, et al. Outcomes of an inpatient medical nutritional rehabilitation protocol in children and adolescents with eating disorders. *J Eat Disord* 2017;5:7.
14. Garber AK, Michihata N, Hetnal K, et al. A prospective examination of weight gain in hospitalized adolescents with anorexia nervosa on a recommended refeeding protocol. *J Adolesc Health* 2012;50:24-29.
15. Golden NH, Keane-Miller C, Sainani KL, et al. Higher caloric intake in hospitalized adolescents with anorexia

- nervosa is associated with reduced length of stay and no increased rate of refeeding syndrome. *J Adolesc Health* 2013;53:573-578.
16. de Zwaan M, Aslam Z, Mitchell JE. Research on energy expenditure in individuals with eating disorders: a review. *Int J Eat Disord* 2002;31:361-369.
 17. Butte NF, Treuth MS, Mehta NR, et al. Energy requirements of women of reproductive age. *Am J Clin Nutr* 2003;77:630-638.
 18. Hasegawa A, Usui C, Kawano H, et al. Characteristics of body composition and resting energy expenditure in lean young women. *J Nutr Sci Vitaminol (Tokyo)* 2011;57:74-79.
 19. Roberts SB, Dallal GE. Energy requirements and aging. *Public Health Nutr* 2005;8:1028-1036.
 20. Black AE, Coward WA, Cole TJ, et al. Human energy expenditure in affluent societies: an analysis of 574 doubly-labelled water measurements. *Eur J Clin Nutr* 1996;50:72-92.
 21. Onur S, Haas V, Bosy-Westphal A, et al. L-tri-iodothyronine is a major determinant of resting energy expenditure in underweight patients with anorexia nervosa and during weight gain. *Eur J Endocrinol* 2005;152:179-184.
 22. Moshang T Jr, Parks JS, Baker L, et al. Low serum triiodothyronine in patients with anorexia-nervosa. *J Clin Endocrinol Metab* 1975;40:470-473.
 23. Croxson MS, Ibbertson HK. Low serum triiodothyronine (T3) and hypothyroidism in anorexia nervosa. *J Clin Endocrinol Metab* 1977;44:167-174.
 24. Reinehr T, Isa A, de Sousa G, et al. Thyroid hormones and their relation to weight status. *Horm Res* 2008;70:51-57.
 25. Dubois EF. Basal metabolism in health and disease. 3rd ed. Philadelphia: Lea and Febiger; 1936.
 26. Belizer CM, Vagedes J. High-resolution infrared body surface temperature and self-perceived warmth distribution in adolescent anorexia nervosa patients. *Journal of Psychophysiology* 2019;33:139-147.
 27. Smith DK, Ovesen L, Chu R, et al. Hypothermia in a patient with anorexia nervosa. *Metabolism* 1983;32:1151-1154.
 28. Van Wymelbeke V, Brondel L, Brun JM, et al. Factors associated with the increase in resting energy expenditure during refeeding in malnourished anorexia nervosa patients. *Am J Clin Nutr* 2004;80:1469-1477.
 29. Rosen E, Sabel AL, Brinton JT, et al. Liver dysfunction in patients with severe anorexia nervosa. *Int J Eat Disord* 2016;49:151-158.
 30. Hanachi M, Melchior JC, Crenn P. Hypertransaminasemia in severely malnourished adult anorexia nervosa patients: risk factors and evolution under enteral nutrition. *Clin Nutr* 2013;32:391-395.
 31. Porcelli P, Leandro G, De Carne M. Functional gastrointestinal disorders and eating disorders. Relevance of the association in clinical management. *Scand J Gastroenterol* 1998;33:577-582.
 32. Robinson PH, Clarke M, Barrett J. Determinants of delayed gastric emptying in anorexia nervosa and bulimia nervosa. *Gut* 1988;29:458-464.
 33. Sato Y, Fukudo S. Gastrointestinal symptoms and disorders in patients with eating disorders. *Clin J Gastroenterol* 2015;8:255-263.
 34. Norris ML, Harrison ME, Isserlin L, et al. Gastrointestinal complications associated with anorexia nervosa: a systematic review. *Int J Eat Disord* 2016;49:216-237.
 35. Caregato L, Di Pascoli L, Favaro A, et al. Sodium depletion and hemoconcentration: overlooked complications in patients with anorexia nervosa? *Nutrition* 2005;21:438-445.
 36. Ehrlich S, Querfeld U, Pfeiffer E. Refeeding oedema: an important complication in the treatment of anorexia nervosa. *Eur Child Adolesc Psychiatry* 2006;15:241-243.
 37. Rigaud D, Boulier A, Tallonneau I, et al. Body fluid retention and body weight change in anorexia nervosa patients during refeeding. *Clin Nutr* 2010;29:749-755.
 38. Mewes R, Tagay S, Senf W. Weight curves as predictors of short-term outcome in anorexia nervosa inpatients. *Eur Eat Disord Rev* 2008;16:37-43.
 39. Gaudiani JL, Brinton JT, Sabel AL, et al. Medical outcomes for adults hospitalized with severe anorexia nervosa: an analysis by age group. *Int J Eat Disord* 2016;49:378-385.
 40. Makhzoumi SH, Coughlin JW, Schreyer CC, et al. Weight gain trajectories in hospital-based treatment of anorexia nervosa. *Int J Eat Disord* 2017;50:266-274.
 41. American Psychiatric A FD. Diagnostic and statistical manual of mental disorders. 5th ed. Washington DC: American Psychiatric Association; 2013.
 42. US National Cancer Institute (NCI). Common Terminology Criteria for Adverse Events (CTCAE) Version 5.0. Washington DC: US Department of Health and Human Services; 2017.
 43. DAT Southgate. The relationship between food composition and available energy. Provisional Agenda Item

- 4.1.3. Joint FAO/WHO/UNU Expert Consultation on Energy and Protein Requirements; 1981 Oct 5-17; Rome: Food and Agriculture Organization of the United Nations, World Health Organization, The United Nations University.
44. Forbes GB. Influence of nutrition. Human body composition. Growth, aging, nutrition, and activity. Springer-Verlager, New York; 1987.
45. Miyake R, Tanaka S, Ohkawara K, et al. Validity of predictive equations for basal metabolic rate in Japanese adults. *J Nutr Sci Vitaminol (Tokyo)* 2011;57:224-232.
46. Long CL, Schaffel N, Geiger JW, et al. Metabolic response to injury and illness: estimation of energy and protein needs from indirect calorimetry and nitrogen balance. *JPEN J Parenter Enteral Nutr* 1979;3:452-456.
47. Jésus P, Ouelaa W, François M, et al. Alteration of intestinal barrier function during activity-based anorexia in mice. *Clin Nutr* 2014;33:1046-1053.
48. Yamashita S, Kawai K, Yamanaka T, et al. BMI, body composition, and the energy requirement for body weight gain in patients with anorexia nervosa. *Int J Eat Disord* 2010;43:365-371.
49. Takamata A. Modification of thermoregulatory response to heat stress by body fluid regulation. *The Journal of Physical Fitness and Sports Medicine* 2012;1:479-489.
50. Kinney JM, Long CL, Gump FE, et al. Tissue composition of weight loss in surgical patients. I. Elective operation. *Ann Surg* 1968;168:459-474.
51. Barak N, Wall-Alonso E, Sitrin MD. Evaluation of stress factors and body weight adjustments currently used to estimate energy expenditure in hospitalized patients. *JPEN J Parenter Enteral Nutr* 2002;26:231-238.
52. Nozoe S, Soejima Y, Yoshioka M, et al. Clinical features of patients with anorexia nervosa assessment of factors influencing the duration of in-patient treatment. *J Psychosom Res* 1995;39:271-281.

Primarily Outcome Report of Our Updated Structural Strategy for Treating Patients with Acute Respiratory Distress Syndrome Following Corona Virus Disease 2019 during the Third Pandemic Phase in Japan

KENICHIRO UCHIDA, KENJI MATSUO, SAE KAWATA, AYAKO KIRITOSHI, RYO DEGUCHI, HOSHI HIMURA, MASAHIRO MIYASHITA, KATSUMI YAMAMOTO, SHINICHIRO KAGA, TOMOHIRO NODA, TETSURO NISHIMURA, HIROMASA YAMAMOTO, and YASUMITSU MIZOBATA

*Department of Traumatology and Critical Care Medicine,
Osaka City University Graduate School of Medicine*

Abstract

Background

The management of acute respiratory distress syndrome (ARDS) induced by corona virus disease 2019 (COVID-19) continues to be challenging, and mortality remains uncontrolled in several countries. After the first and second pandemic phases during approximately March 2020 to June 2020 in Japan, the in-hospital mortality of our patients with ARDS remained high at 33.3%, so we updated and modified our treatment strategy. The aim of this study was to assess our institutional treatment strategy and its outcomes in the third pandemic phase of COVID-19 in Japan.

Methods

This was a single-center, retrospective study, and all patients admitted during October 2020 to March 2021 due to ARDS following COVID-19 were reviewed.

Results

During the study period, 56 patients were managed under mechanical ventilation due to COVID-19 concomitant with ARDS. Their median age was 73 (66-80) years old and 67.9% were male. The P/F ratio at the time of admission was 170 (132-222). The median Sequential Organ Failure Assessment score was 12 (12-14), and two patients required extracorporeal membrane oxygenation. Our modified structural strategy with aggressive administration of muscle relaxant drugs to prevent self-inflicted lung injury achieved extubation in 30 patients and successfully weaned from ventilation in 36 patients. The total in-hospital mortality rate during the study period was 16.1%.

Conclusions

Our modified intensive care strategy for ARDS following COVID-19 achieved improved outcomes.

Received March 24, 2021; accepted June 8, 2021.

Correspondence to: Kenichiro Uchida, MD, PhD, FACS.

Department of Traumatology and Critical Care Medicine, Osaka City University Graduate School of Medicine, 1-4-3 Asahimachi, Abeno-ku, Osaka 545-8585, Japan

Tel: +81-6-6645-3987; Fax: +81-6-6646-3988

E-mail: cvs.uchida@gmail.com

Preventing self-inflicted lung injury by using muscle relaxant drugs appears to be a key tactic once patients require mechanical ventilatory support.

Key Words: ARDS; COVID-19; Mortality; Muscle relaxant drugs; P-SILI

Introduction

The management of severe acute respiratory distress syndrome (ARDS) induced by corona virus disease 2019 (COVID-19) continues to be a difficult situation, and mortality remains uncontrolled in several countries^{1,2}. During the first and second pandemic phases from approximately March 2020 to June 2020 in Japan, we managed the severity of compromised patients especially by taking care to prevent ventilator-associated lung injury as globally prescribed³⁻⁵, but it was sometimes difficult to control self-inspiration efforts of the patients, which resulted in hyper tidal volume ventilation even though peak intratracheal pressure was controlled. In the previous pandemic phase in Japan, final in-hospital mortality after following our institutional stepwise strategy for ARDS following COVID-19 was high at 33.3%⁶. To improve this rate, and because some previous reports recommended prioritization of controlling patient self-inflicted lung injury (P-SILI) in ARDS management⁷⁻⁹, we modified our respiratory management strategy to aggressively administer muscle relaxant drugs to limit spontaneous breathing. The aim of this study was to assess our updated treatment approach for the patients with ARDS related to COVID-19.

Methods

In this single-center, retrospective review, we assessed the records of all patients who had been admitted to the Trauma and Critical Care Center of Osaka City University Hospital because of a severe respiratory condition following COVID-19 from October 2020 to March 2021. We excluded the patients who had not needed mechanical ventilation support entirely or who had been in cardiopulmonary arrest (systolic blood pressure <40 mm Hg) on arrival to hospital. The patients who were intubated and placed on positive mechanical ventilation because of ARDS were reviewed and evaluated for outcomes and complications. The classification of ARDS severity was according to the Berlin definition¹⁰. An outline of our modified stepwise treatment approach for ARDS following COVID-19 is shown in Figure 1.

Treatment for COVID-19

In this third domestic pandemic phase, for the patients with polymerase chain reaction (PCR)-positive severe acute respiratory syndrome coronavirus 2 (SARS-CoV-2) infection, we basically use remdesivir for the ARDS patients and favipiravir for the patients with decreased renal function or chronic kidney disease. Remdesivir was administered at an initial dose of 200 mg on the first day and continued at 100 mg per day for the next 10 days^{11,12}. The initial dose of favipiravir was 3600 mg on the first day and 1600 mg per day for the next 14 days¹³.

Considering the potential for the patients to acquire community-acquired pneumonia, ceftriaxone was administered concomitantly until the sputum culture was confirmed. At the time the sputum culture was confirmed to be negative or show normal flora, we terminated this antibiotic, and if causative bacteria such as methicillin-resistant *Staphylococcus aureus* were detected or had already been detected at the previous hospital, we added or continued drugs susceptible for these bacteria.

Respiratory management focusing on patient self-inflicted lung injury

During the previous first and second pandemic phases, as there were many reports warning of

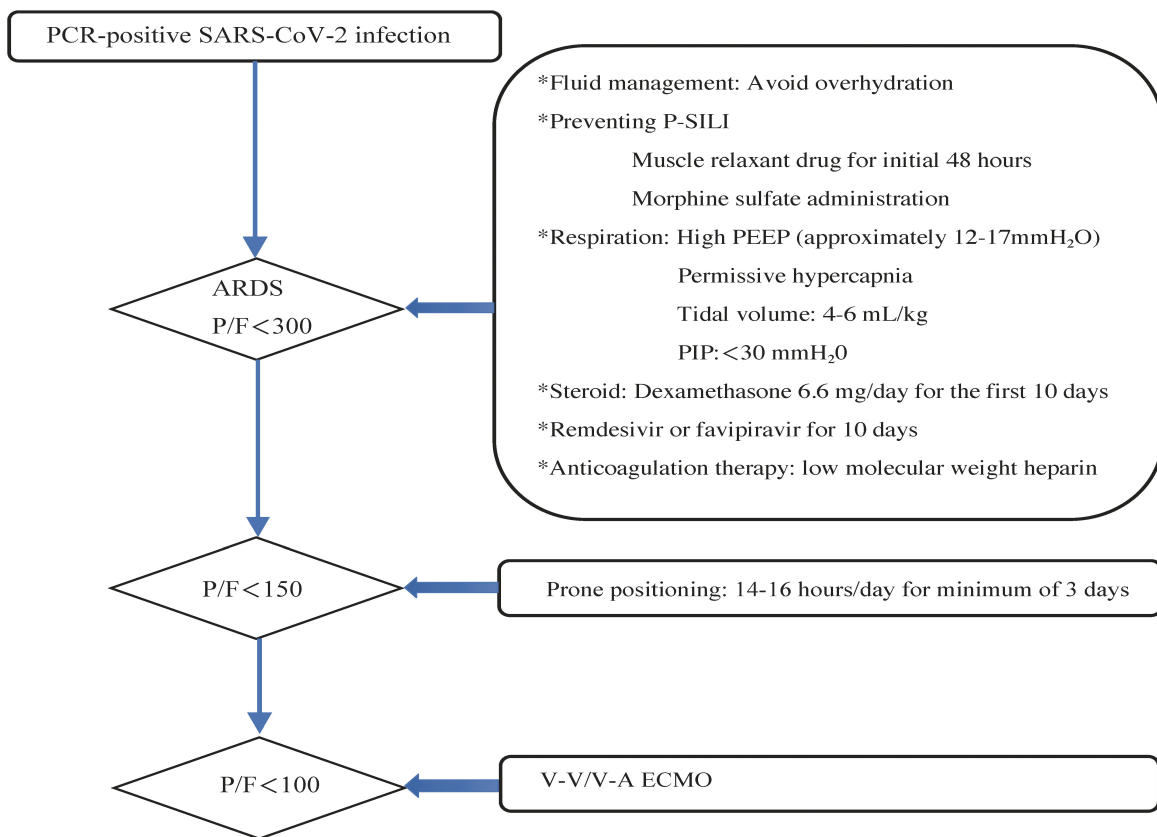


Figure 1. Our stepwise approach to treating ARDS secondary to COVID-19. ARDS, acute respiratory distress syndrome; PCR, polymerase chain reaction; SARS-CoV-2, severe acute respiratory syndrome coronavirus 2; P-SILI, patient self-inflicted lung injury; PEEP, positive end-expiratory pressure; P/F, $\text{PaO}_2/\text{FiO}_2$ ratio; PIP, positive inspiratory pressure; and V-V/V-A ECMO, veno-venous/veno-arterial extracorporeal membrane oxygenation.

adverse complications of thromboembolism as a result of hyper-coagulopathic issues related to COVID-19¹⁴⁻¹⁶), we dared to taper sedative drugs once a day to assess the level of consciousness and to evaluate neurological deficits of the patients. In the current study period, however, we converted to a strategy of preventing P-SILI as much as possible by administering muscle relaxant drugs for the first 48 hours of ventilatory support. During this period, the spontaneous respiration of the patients was completely suppressed and intratracheal pressure was strictly monitored. However, if the patients had already been clearly concomitant with aspiration pneumonia or under hemodynamically unstable at the time of admission, we did not dare to administrate muscle relaxant drugs for these patients. The tidal volume was strictly limited to under 6 mL/kg of ideal body weight by using the pressure-regulated volume control (PRVC) ventilation mode^{4,17}. To prevent the occurrence of ventilator-induced lung injury, maximum airway pressure was controlled so as not to exceed 30 cm H_2O ¹⁸. After muscle relaxant drugs were stopped, if the patients showed poor synchronization with the ventilator, fentanyl was replaced with morphine sulfate 0.6 mg/kg/hour to control excess spontaneous respirations. We additionally monitored both static and dynamic lung compliance and also airway occlusion pressure at 100 msec ($P_{0.1}$), which allowed us to evaluate the inspiratory efforts of the patients during spontaneous respiration. If the patient required mechanical ventilatory support for more than 14 days, we performed a tracheostomy and continued to try weaning the patient ventilation support.

Infusion management

Infusion control was based on serum lactate level, maintenance of stroke volume variation between a range of 10%-18%, and maintenance of the length of the left ventricular enddiastolic diameter between a range of 35-40 mm and that of the inferior vena cava diameter between a range of 8-15 mm as measured via echocardiography.

If we could not obtain a sufficient mean atrial pressure despite maintaining intravenous volume, norepinephrine and/or dobutamine was administered based on the patient's cardiac function. If the administration speed of norepinephrine exceeded 0.1 µg/kg/h, we considered adding vasopressin to control systemic peripheral vascular resistance.

Prolonged prone positioning for a minimum of three days

If a PaO₂/FiO₂ (P/F) ratio ≥150 could not be obtained even under maximum appropriate ventilatory support, aggressive prone position therapy was introduced especially for patients with a computed tomography (CT) finding of type H COVID-19 infection¹⁹. To obtain the maximum effect from this treatment, the prone position was continued for >14 hours but <16 hours to avoid complications such as pressure ulcers^{20,21}. In the previous pandemic phase, we sometimes discussed about how many days the prone position should be continued, and we ultimately decided to continue it for a minimum of three days if the patient was a candidate for this treatment.

Administration of extracorporeal membrane oxygenation (ECMO)

In patients in whom a P/F ratio of >100 could not be obtained even with the addition of prone position therapy and there were no absolute contraindications in the patients, we started them on veno-venous ECMO as an additional treatment option.

Use of dexamethasone

In the previous pandemic phases, we generally used low-dose methylprednisolone at 1 mg/kg/day if the patient met the diagnostic criteria for the acute phase of ARDS. But on the basis of current reports^{22,23}, we converted to the routine administration of dexamethasone at 6.6 mg/day for the first 10 days for the patients requiring oxygen inhalation or mechanical ventilation.

Prophylactic administration of low molecular weight heparin

If there were no hemorrhagic complications on admission, we started low molecular weight heparin from the first day of admission because of reports of a high incidence of complications of hypercoagulopathy specific to COVID-19¹⁴⁻¹⁶. If the patients were complicated by disseminated intravascular coagulopathy (DIC) as calculated by the acute DIC score during their clinical course²⁴, we converted them to the use of recombinant human soluble thrombomodulin and added antithrombin III if the value in the blood was <70%.

Periodic assessment of lung with computed tomography

In the previous phases, to avoid nonessential transport and supervenient infection, we avoided performing periodic radiographic assessment of the lung by CT scan. Sometimes however, fibrotic change of the lung in the late stage or pale ground-glass opacity of the dorsal lung was quite difficult to detect on portable chest x-ray images, so we decided to send the patient for a CT scan approximately 7 days after admission, and strategic decision making was reconsidered on the basis of the CT findings.

Nutrition management

During the previous pandemic phases, we continuous enteral nutrition support as much as possible even if the patient was in the prone position. But sometimes the patients, and especially

those in the prone position, vomited massively, and complications of aspiration pneumonia exacerbated their respiratory condition. Hence, in the current study period, enteral nutrition for the patients placed in prone positioning was administered only when they were in the supine position. Furthermore, we strictly monitored gastric residual volume, and high caloric parenteral nutrition was concurrently administered to these patients.

Statistical analysis

Statistical values are expressed as the median (interquartile range 25%-75%) or number (%).

Results

From October 2020 to March 2021, 70 patients were hospitalized with PCR-positive SARS-CoV-2 infection. We excluded 13 patients who did not require full management with mechanical ventilation and one patient who had been transferred in cardiopulmonary arrest on arrival. Finally, 56 patients who met the criteria for ARDS based on the Berlin definition and were managed with mechanical ventilation were evaluated.

The previous medical histories of the patients at the time of admission are shown in Table 1. Their median age was 73 (66-80) years old, and 38 patients (67.9%) were male. The number of days from disease onset to admission to our hospital was 8 (6-11) days. The median Sequential Organ Failure Assessment score at the time of intensive care unit (ICU) admission was calculated as 12 (12-14).

The results of the main blood tests and radiological types of COVID-19 infection obtained at the time of ICU admission are shown in Table 2. The P/F ratio at the time of ICU admission was 170 (132-222), and 18 (32.1%) patients had already been intubated at a previous hospital. Lactate dehydrogenase on admission was 424 (368-496) IU/L, Krebs von der Lungen 6 was 466 (132-676) U/mL, and C-reactive protein was 7.5 (4.1-14.4) mg/dL. Nine (16.1%) patients were classified by CT scan to have Type L COVID-19 infection, which shows only ground-glass densities to be present, and 47 (83.9%) patients had Type H infection, which shows a remarkable increase in lung weight especially in the dorsal side of the bilateral lungs. The median value of $P_{0.1}$ in the intubated patients on admission was 1.1 (0.6-1.7) cmH₂O, and lung dynamic compliance was decreased to 31 (24-35) mL/cmH₂O.

The details of the clinical data are listed in Table 3. Although none of the patients had been in shock requiring vasopressors in the previous hospital, 49 (87.5%) of the patients required vasopressors mainly due to the use of deep sedation concomitant with muscle relaxant drugs. Prone position therapy, which was performed for approximately 16 (15.5-17) hours/day, was administered in 22 (39.3%) patients. The concomitant complications observed during admission were ventilator-associated pneumonia in 20 patient (35.7%), gastrointestinal bleeding requiring blood transfusion in two patients (3.6%), and mediastinal emphysema or pneumothorax in three patients (5.4%). Seven patients (12.5%) had a systemic fungal infection for which they were administered anti-fungal drugs on the basis of their β -D-glucan value, and *Clostridioides difficile* infection was present in five (8.9%) patients. One patient had undergone cricothyrotomy because of endotracheal tube obstruction on the 12th day after admission. A tracheostomy was subsequently performed in this patient, who was successfully weaned from mechanical ventilation and whose cerebral performance category score was good.

ECMO therapy was indicated in two patients based on their P/F ratio on admission and Type L radiographic findings. These two patients were managed by ECMO for 10 days and 14 days respectively, and both patients were successfully extubated with no complications. Renal replacement

Table 1. Patient demographic data

	N=56
Sex, Male	38 (67.9%)
Age, years	73 (66-80)
Transferred from other hospital	52 (92.9%)
Onset to admission time (days)	8 (6-11)
Physiological data on arrival	
GCS	15 (3-15)
Respiratory rate (breaths per min)	25 (20-30)
Heart rate (beats per min)	88 (77-102)
Systolic blood pressure (mm Hg)	148 (131-158)
Body temperature (°C)	36.4 (36.2-36.9)
Past medical history/Underlying disease	
Current/Ex-smoker	20 (35.7%)
Alcohol abuser	4 (7.1%)
Hypertension	48 (85.7%)
Diabetes	29 (51.8%)
Hyperlipidemia	24 (42.8%)
Stroke	8 (14.3%)
Cardiac failure	5 (8.9%)
COPD	5 (8.9%)
Chronic kidney disease	7 (12.5%)
Asthma	4 (7.1%)
Obesity	9 (16.1%)
Malignant Disease	14 (25.0%)
Gout	7 (12.5%)
Psychological illness	3 (5.4%)
Respiratory condition	
ARDS	56
Mild	20 (35.7%)
Moderate	31 (55.4%)
Severe	5 (8.9%)
SOFA score on ICU admission	12 (12-14)

Statistical data are presented as median (25%-75% interquartile range) or number. GCS, Glasgow Coma Scale; COPD, chronic obstructive pulmonary disease; ARDS, acute respiratory distress syndrome; SOFA, Sequential Organ Failure Assessment; and ICU, intensive care unit.

therapy was administered in six (10.7%) patients due to their chronic kidney disease on dialysis and one patient (1.8%) due to acute kidney injury.

Recovery from ARDS and successful extubation was achieved in 30 patients (53.6%) over 8 (6-11) days, and they were transferred to another hospital. Their dynamic lung compliance just before extubation had improved to 62 (56-72) mL/cmH₂O in the extubated patients. Tracheostomy was performed in 24 (42.9%) patients, and five patients were successfully weaned from mechanical ventilatory support. The obtained cerebral performance category score of the patients at the point of disposition was 1 in thirty-eight patients (67.9%), 2 in eight (14.3%), 3 in one (1.8%), 4 in zero, and 5 in nine patients (16.1%). During this third pandemic study period, final in-hospital mortality was 16.1% (9/56 patients).

Table 2. Examination results at the time of ICU admission

	N=56
P/F ratio	170 (132-222)
P _{0.1}	1.1 (0.6-1.7)
Dynamic lung compliance	31 (24-35)
PaCO ₂	42.4 (34.1-52.2)
Base excess	-0.5 (-2.6-1.5)
pH	7.397 (7.301-7.469)
Lactate level (mmol/L)	1.2 (0.9-1.6)
WBC (/μL)	8850 (5800-13000)
Plt (×10 ⁴ /μL)	21.2 (15.0-27.0)
CRP (mg/dL)	7.5 (4.1-14.4)
Cr (mg/dL)	0.74 (0.59-1.14)
BUN (mg/dL)	22.5 (17.5-33.5)
CK (IU/L)	71 (33-173)
LDH (IU/L)	424 (368-496)
KL-6 (U/mL)	466 (132-676)
HgbA1c (%)	6.3 (5.9-6.8)
T-Bil (mg/dL)	0.5 (0.4-0.7)
Fibrinogen (mg/dL)	531 (449-643)
FDP (μg/mL)	6.8 (4.5-10.8)
Type of COVID-19 infection classified by CT scan	
Type L	9 (16.1%)
Type H	47 (83.9%)

Statistical data are presented as median (25%-75% interquartile range). ICU, intensive care unit; P/F, PaO₂/FiO₂; WBC, white blood cell count; Plt, platelet count; CRP, C-reactive protein; Cr, creatinine; BUN, blood urea nitrogen; CK, creatine kinase; IU/L, international unit; LDH, lactate dehydrogenase; KL-6, Krebs von der Lungen 6; HgbA1c, hemoglobin A1c; T-Bil, total bilirubin; FDP, fibrinogen degradation products; and CT, computed tomography.

Discussion

Ever since the first pandemic of COVID-19 occurred in 2019²⁵⁾, treatment strategies for COVID-19 and the related ARDS have been documented globally and updated as clinical recommendations²³⁾. Currently, however, we still lack radical antiviral treatment agents to treat this human crisis^{25,26)}. The respiratory management of ARDS has been discussed globally for some time^{4,17,27)}. Generally, high positive end-expiratory pressure (PEEP) and low tidal volume to prevent shearing injury of the alveoli are considered important in the management to rest the lungs, but methods to control and limit spontaneous inspiratory effort have not been established yet. To control these self-inspiratory efforts, we use muscle relaxant drugs as the treatment option for ARDS patients. However, the administration of muscle relaxant drugs to control self-inspiratory efforts and oxygen consumption of patients suffering ARDS remains controversial^{10,28)}. Papazian et al¹⁰⁾ previously reported the importance of muscle relaxant drugs for patients with ARDS. They used muscle relaxant drugs for about 48 hours for their patients with a P/F ratio of under 150 and reported a 32% decrease in 90-day mortality and decreases in the number of ventilator days and intensive care unit admission days. In contrast, Putensen et al²⁹⁾ reported that maintaining spontaneous breathing and adopting airway pressure release ventilation obtained good outcomes as well. Our previous management strategy, which was similar to this strategy of maintaining spontaneous breathing, did not result in excellent

Table 3. Clinical courses

	N=56
Successful extubation	30 (53.6%)
Length of ventilator support from admission, days	8 (6-11)
Length of stay in ICU, days	10 (6.5-13.5)
Dynamic lung compliance before extubation	62 (56-72)
Tracheostomy	24 (42.9%)
Length of ventilator support from admission, days	18 (16-21)
Length of stay in ICU, days	18.5 (16-22)
Dynamic lung compliance before tracheostomy	32 (26-34)
Required prone positioning	22 (39.3%)
Length of prone positioning days (days)	3 (3-5)
Length of prone positioning hours per day (hours)	16 (15.5-17)
Required blood transfusion	8 (14.3%)
Steroid use	56 (100%)
Muscle relaxant use	49 (87.5%)
Vasopressor use	49 (87.5%)
CRRT	7 (12.5%)
ECMO	2 (3.6%)
Tracheostomy/Cricothyrotomy	22 (39.3%)/1 (1.8%)
Concomitant comorbidities during admission	
Pneumothorax	2 (3.6%)
Mediastinal emphysema	1 (1.8%)
Ventilator associated pneumonia	20 (35.7%)
Endotracheal re-intubation	1 (1.8%)
Acute kidney injury requiring CRRT	1 (1.8%)
Gastrointestinal bleeding	2 (3.6%)
Deep venous thrombosis	1 (1.8%)
Systemic fungal infection	7 (12.5%)
Mild pressure sore (prone-positioned patient)	2 (3.6%)
<i>Clostridioides difficile</i> infection	5 (8.9%)
CPC grade obtained on disposition	
I	38 (67.9%)
II	8 (14.3%)
III	1 (1.8%)
IV	0
V	9 (16.1%)
In-hospital mortality	9 (16.1%)

Statistical data are presented as median (25%-75% interquartile range) or number. ICU, intensive care unit; CRRT, continuous renal replacement therapy; ECMO, extracorporeal membrane oxygenation; and CPC, Cerebral Performance Category.

outcomes for ARDS following COVID-19⁶. We consider that one reason for this outcome arose from not preventing P-SILI. Self-inflicted lung injury is also being re-emphasized in the management of COVID-19 because the huge inspiratory efforts to correct hypoxia cause additional shearing injury of the alveoli^{4,16}. Administration of deep sedation and concomitant use of muscle relaxant drugs are efficient to avoid P-SILI, but the difficulty in preferentially addressing this problem in COVID patients is that we cannot assess complications of thromboembolic events such as cerebral infarction during the administration of muscle relaxant. By administering anticoagulant drugs from the first

days of admission and continuous daily checking of the values of coagulation factors such as fibrinogen degradation products (FDP), we could prevent thromboembolic events during this period.

Furthermore, the importance of monitoring airway pressure including transpulmonary pressure is currently being emphasized, but there are still no strong recommendations for the respiratory management of COVID-19-related ARDS. From our experience in the previous pandemic phases, during which we struggled with how to manage spontaneous inspiratory efforts of the intubated patients, we start monitoring $P_{0.1}$, which allows us to estimate inspiratory effort of the patients even though respiratory muscle weakness may be present^{4,30-32}. As the value of $P_{0.1}$ at the time of ICU admission was scored under deep sedation with muscle relaxant drugs, hence the value was considered to have been well regulated. Similarly, during the administration of muscle relaxant drugs, $P_{0.1}$ is well controlled under 5 cmH₂O, and this is one of the important reasons we could obtain good outcomes in the present study period. Under use of muscle relaxant drugs, the respiratory drive of all of our patients was well controlled by PRVC ventilation, and the intratracheal pressure was also controlled under 30 mmH₂O, regardless of whether the patients had a massive type L or H radiographic appearance. And also, after muscle relaxant drugs being terminated, the administration of morphine sulfate seemed effective to control excess spontaneous respirations and the respiration of the patients was well synchronized to the ventilator support compared to fentanyl.

As additional treatment, especially for the patients with type H appearance, we considered the strategies combining prone positioning and muscle relaxant treatment with PRVC ventilation to be efficient. However, in the patients with type L appearance, the prone position does not adequately correct V/Q mismatch, so we aggressively applied veno-venous (V-V) ECMO if the patient had not obtained improvement under best ventilatory support. We applied V-V ECMO in two patients during the present study period, and both were successfully weaned from ECMO, extubated, and transferred to a rehabilitation hospital.

The use of remdesivir as an anti-viral drug, which we used continuously during the study period, is controversial, and WHO also reported that there were no strong recommendations for using this drug²³. However, as there are currently no established anti-viral drugs against COVID-19, we will continue to use remdesivir for all patients except those with renal failure.

Another key modification of our strategy against ARDS following COVID-19 was in converting from the previous use of low-dose methylprednisolone to the use of dexamethasone. Although dexamethasone appeared to be efficient in the treatment of ARDS during the present study period as well, because of its long-term use of approximately 10 days, it caused some adverse side effects, especially in terms of infection control. We will need to assess the efficacy of dexamethasone use in upcoming multi-institutional randomized control trials.

Lastly, since no complication such as cerebral hemorrhage or cerebral infarction had been detected during their admission, the obtained CPC score of 2 and 3 were presumed because of sedative coma but had to be transferred to rehabilitation hospital before their awakening.

Although the present descriptive statistical outcomes are reported from a small number of patients at a single institution, our modified systematic stepwise intensive care strategy for treating ARDS secondary to COVID-19 in the third pandemic period in Japan improved patient outcomes compared to those in the previous two pandemic phases.

We conclude that our modified systematic stepwise strategy of intensive care for treating ARDS secondary to COVID-19 used in the third phase of the pandemic in Japan achieved improved

outcomes compared to the high mortality rates seen around the world including elsewhere in Japan.

After we had updated our treatment strategy on the basis of global evidence, several important tactical changes including in respiratory management had been made after the first and second domestic pandemic periods. Hence, we realize that numerous co-variants need to be analyzed to determine which factors significantly impacted the current descriptive statistical outcomes. Furthermore, as the number of patients who can be analyzed with propensity-matched analysis is currently insufficient, as the next step, we definitely need to evaluate which co-factors are the most efficient in improving our short-term outcomes of ARDS following COVID-19. We are currently proceeding with a multi-institutional randomized control trial to reassess our outcomes on the basis of the present study.

Acknowledgements

All authors have no COI to declare regarding the present study.

Written informed consent for this report was obtained from the patients or their family members.

We sincerely dedicate this paper to all essential health workers who have fought against COVID-19 not only directly but also secondarily in Osaka City University Hospital. The excellent results are due to the tremendous cooperation and teamwork of all of the staff involved in such tasks as preventing nosocomial infections, redistributing staff, and temporarily limiting elective operations.

References

1. Baud D, Qi X, Nielsen-Saines K, et al. Real estimates of mortality following COVID-19 infection. *Lancet Infect Dis* 2020;20:773.
2. Johns Hopkins University and Medicine. Mortality analysis. Mortality in the most affected countries. <https://coronavirus.jhu.edu/data/mortality>. Accessed January 15, 2021.
3. Abdallat M, Khalil M, Al-Awwa G, et al. Barotrauma in COVID-19 patients. *J Lung Health Dis* 2020;4:8-12.
4. Griffiths MJD, McAuley DF, Perkins GD, et al. Guidelines on the management of acute respiratory distress syndrome. *BMJ Open Respir Res* 2019;6:e000420.
5. Alhazzani W, Møller MH, Arabi YM, et al. Surviving Sepsis Campaign: guidelines on the management of critically ill adults with Coronavirus Disease 2019 (COVID-19). *Intensive Care Med* 2020;46:854-887.
6. Uchida K, Matsuo K, Kawata S, et al. Systematic stepwise treatment strategy and its short-term outcomes for patients with corona virus disease 2019 complicated by severe acute respiratory distress syndrome. *Osaka City Med J* 2021;67:9-20.
7. Yoshida T, Fujino Y, Amato MBP, et al. Fifty years of research in ARDS. Spontaneous breathing during mechanical ventilation. Risks, mechanisms, and management. *Am J Respir Crit Care Med* 2017;195:985-992.
8. Brochard L, Slutsky A, Pesenti A. Mechanical ventilation to minimize progression of lung injury in acute respiratory failure. *Am J Respir Crit Care Med* 2017;195:438-442.
9. ARDS Definition Task Force; Ranieri VM, Rubenfeld GD, Thompson BT, et al. Acute respiratory distress syndrome: the Berlin definition. *JAMA* 2012;307:2526-2533.
10. Papazian L, Forel JM, Gacouin A, et al. Neuromuscular blockers in early acute respiratory distress syndrome. *N Engl J Med* 2010;363:1107-1116.
11. Beigel JH, Tomashek KM, Dodd LE, et al. Remdesivir for the treatment of Covid-19 - final report. *N Engl J Med* 2020;383:1813-1826.
12. Wang M, Cao R, Zhang L, et al. Remdesivir and chloroquine effectively inhibit the recently emerged novel coronavirus (2019-nCoV) in vitro. *Cell Res* 2020;30:269-271.
13. Chen C, Zhang Y, Huang J, et al. Favipiravir versus Arbidol for COVID-19: a randomized clinical trial. *medRxiv* 2020;03.17.20037432.
14. Zhao J, Rudd A, Liu R. Challenges and potential solutions of stroke care during the coronavirus disease 2019 (COVID-19) outbreak. *Stroke* 2020;51:1356-1357.
15. Klok FA, Kruip MJHA, van der Meer NJM, et al. Confirmation of the high cumulative incidence of thrombotic complications in critically ill ICU patients with COVID-19: an updated analysis. *Thromb Res* 2020;191:148-150.
16. Lodigiani C, Iapichino G, Carenzo L, et al. Venous and arterial thromboembolic complications in COVID-19

- patients admitted to an academic hospital in Milan, Italy. *Thromb Res* 2020;191:9-14.
17. Fan E, Del Sorbo L, Goligher EC, et al. An Official American Thoracic Society/European Society of Intensive Care Medicine/Society of Critical Care Medicine Clinical Practice Guideline: mechanical ventilation in adult patients with acute respiratory distress syndrome. *Am J Respir Crit Care Med* 2017;195:1253-1263.
 18. Slutsky AS, Ranieri VM. Ventilator-induced lung injury. *N Engl J Med* 2013;369:2126-2136.
 19. Gattinoni L, Chiumello D, Caironi P, et al. COVID-19 pneumonia: different respiratory treatment for different phenotypes? *Intensive Care Med* 2020;46:1099-1102.
 20. Guérin C, Reignier J, Richard JC, et al. Prone positioning in severe acute respiratory distress syndrome. *N Engl J Med* 2013;368:2159-2168.
 21. Munshi L, Del Sorbo L, Adhikari NKJ, et al. Prone position for acute respiratory distress syndrome: a systematic review and meta-analysis. *Ann Am Thorac Soc* 2017;14:S280-S288.
 22. RECOVERY Collaborative Group; Horby P, Lim WS, Emberson JR, et al. Dexamethasone in hospitalized patients with Covid-19. *N Engl J Med*. 2021;384:693-704.
 23. World Health Organization. (2020). Clinical management of severe acute respiratory infection when novel coronavirus (2019-nCoV) infection is suspected: interim guidance, 28 January 2020. World Health Organization. <https://apps.who.int/iris/handle/10665/330893> (accessed February 1, 2021).
 24. Gando S, Iba T, Eguchi Y, et al. A multicenter, prospective validation of disseminated intravascular coagulation diagnostic criteria for critically ill patients: comparing current criteria. *Crit Care Med* 2006;34:625-631.
 25. Del Rio C, Malani PN. COVID-19—new insights on a rapidly changing epidemic. *JAMA* 2020;323:1339-1340.
 26. Yang X, Yu Y, Xu J, et al. Clinical course and outcomes of critically ill patients with SARS-CoV-2 pneumonia in Wuhan, China: a single-centered, retrospective, observational study. *Lancet Respir Med* 2020;8:475-481.
 27. Papazian L, Aubron C, Brochard L, et al. Formal guidelines: management of acute respiratory distress syndrome. *Ann Intensive Care* 2019;9:69.
 28. National Heart, Lung, and Blood Institute PETAL Clinical Trials Network; Moss M, Huang DT, Brower RG, et al. Early neuromuscular blockade in the acute respiratory distress syndrome. *N Engl J Med* 2019;380:1997-2008.
 29. Putensen C, Zech S, Wrigge H, et al. Long-term effects of spontaneous breathing during ventilatory support in patients with acute lung injury. *Am J Respir Crit Care Med* 2001;164:43-49.
 30. Telias I, Junhasavasdikul D, Rittayamai N, et al. Airway occlusion pressure as an estimate of respiratory drive and inspiratory effort during assisted ventilation. *Am J Respir Crit Care Med* 2020;201:1086-1098.
 31. Conti G, Antonelli M, Arzano S, et al. Measurement of occlusion pressures in critically ill patients. *Crit Care* 1997;1:89-93.
 32. Telias I, Brochard L, Goligher EC. Is my patient's respiratory drive (too) high? *Intensive Care Med* 2018;44:1936-1939.

An Analysis of Compensatory Trunk Movements in Shoulder Joint Movements: Application to Healthy Individuals and Patients after Shoulder Joint Surgery

TAMOTSU NAKATSUCHI¹⁾, MITSUHIKO IKEBUCHI^{2,4)}, TAKAHIRO NISHINOHARA⁴⁾,
SHIGEYOSHI NAKAJIMA³⁾, and HIROAKI NAKAMURA⁴⁾

*Tsuji-GEKA Rehabilitation Hospital¹⁾;
Department of Rehabilitation medicine²⁾, Osaka City University Hospital;
Department of Electric Information System³⁾,
Osaka City University Graduate School of Engineering; and
Department of Orthopedic Surgery⁴⁾, Osaka City University Graduate School of Medicine*

Abstract

Background

Evaluating upper limb function, particularly shoulder joint kinematics, in activities of daily living is important during rehabilitation. However, an extensive search did not identify any studies investigating the effect of compensatory trunk movements on shoulder joint kinetics using radiographs. Thus, we aimed to compare compensatory trunk movements during shoulder joint kinematics between healthy individuals and patients who had undergone reverse shoulder arthroplasty.

Methods

We included 10 healthy adult shoulders (healthy group) and four shoulders that had undergone reverse shoulder arthroplasty (impaired group). After the attachment of surface markers over the manubrium sterni and spinous process of the third thoracic vertebra to evaluate compensatory trunk movements, participants performed voluntary abduction of the shoulder under fluoroscopy, and the trunk compensation angle was measured on radiographs.

Results

After shoulder abduction of 90°, the healthy group performed compensatory trunk retroflexion, as indicated by the kinematics of the shoulder joint. In the impaired group, at the maximum shoulder abduction position there was lateral flexion of the trunk to the side contralateral to the evaluated shoulder joint and rotation to the side ipsilateral to the evaluated shoulder joint. These findings suggest that compensatory trunk movements occurred in the impaired group in response to reduced shoulder function. Therefore, evaluating compensatory trunk movements over time, in addition to performing range-of-motion and muscle strengthening exercises for improving shoulder joint function,

Received March 11, 2021; accepted August 27, 2021.

Correspondence to: Tamotsu Nakatsuchi, MD, PhD.

Tsuji-GEKA Rehabilitation Hospital,
3-24 Ikutamamaemachi, Tennouji-Ku, Osaka 543-0072, Japan
Tel: +81-6-6771-0681; Fax: +81-6-6773-8647
E-mail: nakatsuchi@kankikai.com

is important in patients undergoing reverse shoulder arthroplasty.

Conclusions

Simultaneous evaluation of the shoulder joint and compensatory trunk movements may provide rehabilitation programs to improve activities of daily living.

Key Words: Compensatory trunk movements; Joint kinetics;
Reverse shoulder arthroplasty; Rehabilitation program

Introduction

In activities of daily living (ADL), upper limb function is important, and the function of the shoulder joint, which is the joint at the base of the upper limb, is particularly important. However, since the movement is complicated, various methods have been used for kinematic analyses to evaluate the function and assess the effects of therapy. Recently, with advances in measuring instruments, various analyses using radiographs have been carried out, and methods of 2D-3D registration that match 3D models, such as computed tomography (CT) and magnetic resonance (MR) images, with 2D models, such as radiographs, have been sporadically observed¹.

The movements of the shoulder joint are carried out jointly via the anatomic joints (the glenohumeral, acromioclavicular, and sternoclavicular joints) and functional joints (the scapulothoracic and second shoulder joints, as well as the trunk, thorax, and lower limbs). If glenohumeral joint mobility is reduced, the scapulothoracic joint compensates to allow mobility; if scapular mobility is reduced, compensatory movements such as anteroposterior flexion, lateral flexion, and rotation of the trunk may occur. However, in our literature search, there were no reports on shoulder joint kinematics that described such compensatory trunk movements during radiographic evaluation, and analyses are thought to have been performed with the implicit understanding that the posture of participants was constant².

In order to accurately perform shoulder joint kinematics analyses, gaining an understanding of the compensatory trunk movements and performing more detailed kinematic analyses were considered necessary. Therefore, in this study, the effects of compensatory trunk movements on shoulder abduction movements were investigated.

We aimed to compare compensatory trunk movements during shoulder joint kinematics between healthy individuals and patients who had undergone reverse shoulder arthroplasty (RSA).

Methods

Ten shoulders from 5 healthy adults with no history of shoulder disease (the healthy group) and four shoulders from four patients who had undergone shoulder arthroplasty (the impaired group) were included in this study. All participants in the healthy group were men, with a mean age of 38.2 ± 11.7 years, and both shoulder joints were evaluated. All participants in the impaired group were women, with a mean age of 75.5 ± 5.6 years, and only the affected shoulders were evaluated. The primary disease in the impaired group was osteoarthritis of the shoulder with rotator cuff tears, and all patients had undergone RSA.

Compensatory trunk movements were measured as the angles of inclination of the thoracic system of coordinates relative to the X-ray system of coordinates, based on frontal chest radiographs in the standing position including the humerus, shoulder joint, scapula, and sternum. The X-ray system of coordinates was defined using the X-ray source as the origin, the perpendicular line from the X-ray

source to the shooting table as the anterior-posterior axis, the vertical line orthogonal to this axis and passing through the origin as the vertical axis, and the axis orthogonal to the anterior-posterior axis and vertical axis and passing through the origin as the horizontal axis.

In the upright position, the upper margin of the sternum is known to be at the same height as the 2nd to 3rd thoracic vertebrae. Using this, the origin was defined as the suprasternal notch *Incisura Jugularis*; the axis passing through the origin and the spinous process of the 3rd thoracic vertebra was the anterior-posterior axis of the thorax, the line connecting the left and right proximal clavicles that is parallel and orthogonal to the anterior-posterior axis and passes through the origin was the horizontal axis, and the axis orthogonal to the anterior-posterior and horizontal axes and passing through the origin was the vertical axis.

The inclination was defined using the angle between the anteroposterior axes of the X-ray and the thoracic systems of coordinates in the horizontal plane as the angle of rotation of the thorax, the angle between the horizontal axes of the X-ray and thoracic systems of coordinates in the frontal plane as the lateral flexion angle of the thorax, and the angle between the anteroposterior axes of the X-ray and thoracic systems of coordinates in the sagittal plane as the anteroposterior flexion angle of the thorax.

Plain radiographs were taken after a cruciform marker (sternum marker) was attached to the suprasternal notch and a ring-shaped marker (spinous process marker) was attached to the spinous process of the 3rd thoracic vertebra. Sternum markers were applied such that the transverse bar passed through the suprasternal notch and was parallel to the line connecting the right and left proximal clavicle ends, and the longitudinal bar was orthogonal to the transverse bar and bisected the sternum. The spinous process markers were applied such that the center of the ring coincided with the spinous process of the 3rd thoracic vertebra (Fig. 1).

With these markers attached, the participants underwent frontal plain radiography with the chest in the upright position. The distance between the source and the imaging plate was set to 100 cm, and the participant's scapula and occipital bone were set to be in contact with the imaging plate. In instances where contact was not feasible due to a hunched back or other reasons, the participant was confirmed to be in an upright position, and the participant was positioned such that the top of the kyphosis was in contact with the imaging plate. If it was still unstable, the participant was seated in a chair and the scapula and occipital region were brought into contact with the imaging plate.

To reproduce the compensatory trunk movements, participants were instructed to perform voluntary abduction movements in increments of 30° from the dropped shoulder position (abduction 0°) and imaging was performed. The maximum abduction angle was set at 180° of abduction and, if abduction of 180° was difficult, the maximum abduction angle which participants could achieve was set as the maximum voluntary abduction angle. The range of motion of voluntary shoulder abduction was measured using a goniometer in accordance with the range of motion and measurement methods defined by the Japanese Orthopaedic Association and the Japanese Association of Rehabilitation Medicine.

Chest thickness (the distance between the sternum and spinous process markers) and the distance between the imaging plate and the spinous process marker in plain radiographs were measured as necessary parameters at the time of imaging. At the measurement, we used the outside caliper for measuring pelvis, and the inside caliper for measuring the inner diameter of pipes, etc.

In terms of ethical considerations, full informed consent was obtained from all participants.

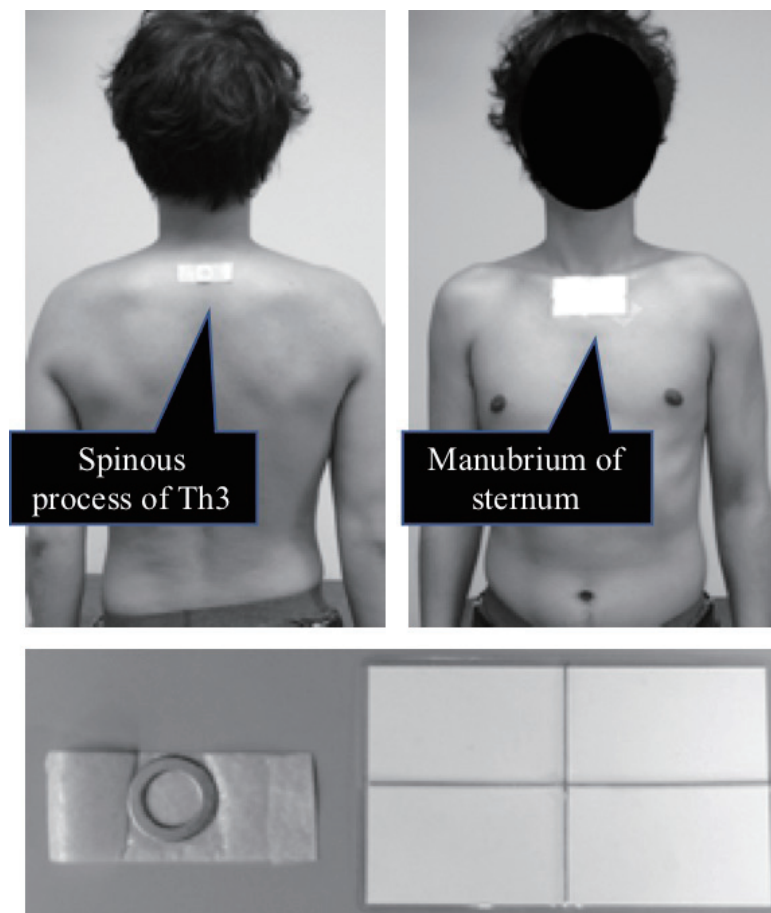


Figure 1. A cruciform marker (Right: sternum marker) was attached to the suprasternal notch and a ring-shaped marker (Left: spinous process marker) was attached to the spinous process of the 3rd thoracic vertebra.

Approval to conduct the research was also obtained from the Institutional Review Board (Approval No. 36).

The following calculation method was devised for evaluating compensatory trunk movements at angles.

X_1 , Y_1 , and Z_1 were set as the coordinates of the spinous process marker in the X-ray system of coordinates, while X_2 , Y_2 , and Z_2 were set as the coordinates of the sternum marker; l_1 is the distance between the imaging plate and the spinous process marker, l_2 is the distance between the imaging plate and the sternum marker, and l_3 is the chest thickness (the distance between the sternum and spinous process markers). L was the distance from the X-ray source to the shooting table, and it was measured to be 1000 mm. On the plain radiographs, the center of the screen was the intersection between the plane containing the imaging plate (IP) and the perpendicular line from the X-ray source, that is, the anterior-posterior axis in the X-ray system of coordinates. In the plain radiographs, the horizontal distance from the center of the screen to the center of the spinous process marker was denoted as x_1 , while the vertical distance was denoted as y_1 ; the horizontal distance from the center of the film to the center of the sternum marker (the intersection of the transverse and longitudinal bars) was denoted as x_2 , and the vertical distance was denoted as y_2 (Fig. 2).

Based on the aforementioned parameters, the spinous process marker coordinates (X_1 , Y_1 , Z_1) were expressed as follows:

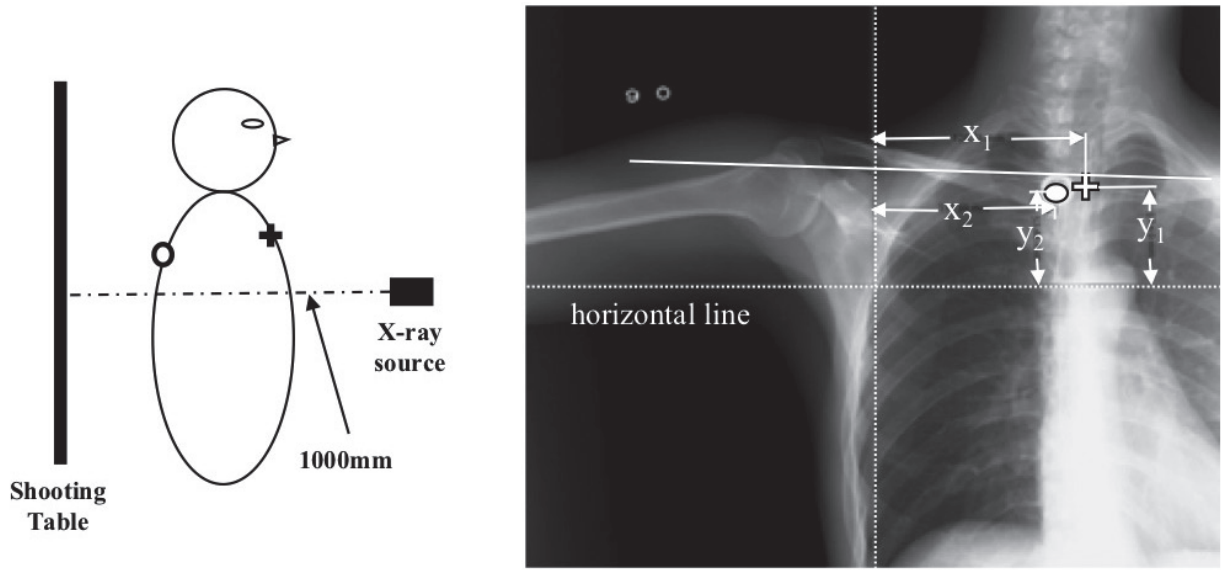


Figure 2. In the plain radiographs, the horizontal distance from the center of the screen to the center of the spinous process marker was denoted as x_1 , while the vertical distance was denoted as y_1 ; the horizontal distance from the center of the film to the center of the sternum marker was denoted as x_2 , and the vertical distance was denoted as y_2 .

Spinous process marker coordinates

$$(X_1, Y_1, Z_1) = (x_1 \cdot (L - l_1) / L, y_1 \cdot (L - l_1) / L, L - l_1) \quad (\text{Formula 1})$$

Similarly, the coordinates of the sternum markers (X_2, Y_2, Z_2) were expressed as follows:

Sternum marker coordinates

$$(X_2, Y_2, Z_2) = (x_2 \cdot (L - l_2) / L, y_2 \cdot (L - l_2) / L, L - l_2) \quad (\text{Formula 2})$$

The chest thickness, that is, the distance between the sternum and spinous process markers (l_3), was calculated as

$$l_3^2 = (X_1 - X_2)^2 + (Y_1 - Y_2)^2 + (Z_1 - Z_2)^2$$

X_1, X_2, Y_1, Y_2, Z_1 , and Z_2 were substituted from Formula 1 and Formula 2. This Formula was the quadratic equation where l_2 represents an unknown.

$$A \cdot l_2^2 + B \cdot l_2 + C = 0$$

$$A = (x_2 / L)^2 + (y_2 / L)^2 + 1$$

$$B = -2 \cdot \{(x_1 / L)(x_2 / L)(L - l_1) + (y_1 / L)(y_2 / L)(L - l_1) + (L - l_1)\}$$

$$C = \{x_1 / L \cdot (L - l_1)\}^2 + \{y_1 / L \cdot (L - l_1)\}^2 + (L - l_1)^2 - l_3^2 \quad (\text{Formula 3})$$

$L, l_1, l_3, x_1, y_1, x_2$, and y_2 were measured values. l_2 was calculated from Formula 3 and substituted into Formula 2 to obtain the sternum marker coordinates (X_2, Y_2, Z_2) (Fig. 3).

Next, the angles of thoracic rotation, anteroposterior flexion, and lateral flexion were calculated. The angle of rotation of the thorax (the angle in the horizontal plane between the anteroposterior axes of the X-ray and thoracic systems of coordinates) was denoted by α ; β denoted the anteroposterior

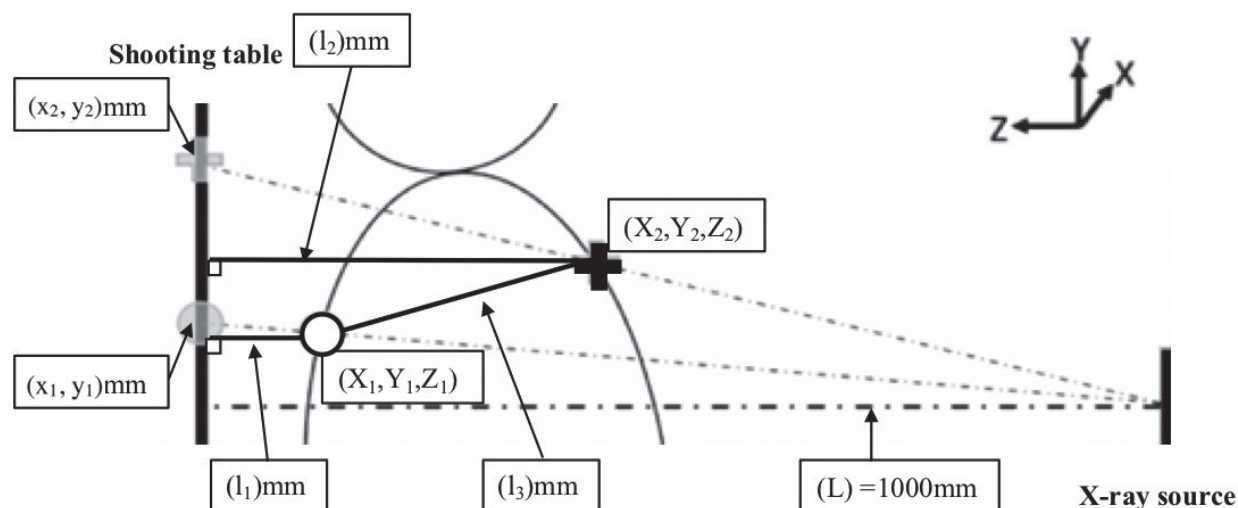


Figure 3. L , l_1 , l_3 , x_1 , y_1 , x_2 , and y_2 were measured values. l_2 was calculated from Formula 3 and substituted into Formula 2 to obtain the sternum marker coordinates (X_2, Y_2, Z_2) .

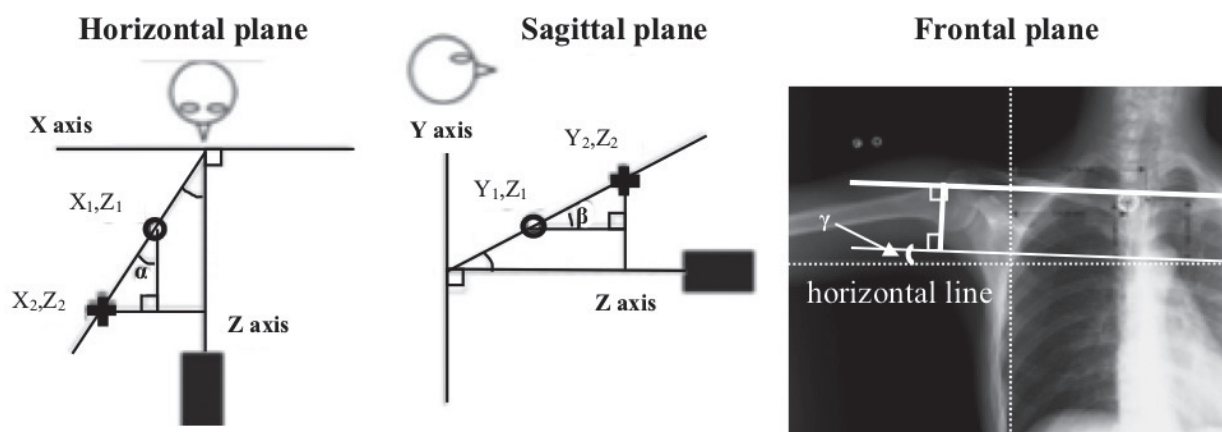


Figure 4. Angles α and β were calculated from formula 4 using the inverse tangent function.

flexion angle of the thorax (the angle between the anteroposterior axes of the X-ray and thoracic systems of coordinates in the sagittal plane), and γ denoted the lateral flexion angle of the thorax (the angle between the horizontal axes of the X-ray and thoracic systems of coordinates in the frontal plane). The angle α was the angle between the projection of the line connecting the sternum and spinous process markers on the horizontal plane and the line connecting the origin of the X-ray system of coordinates and the center of the screen. The angle β was the angle between the projection of the line connecting the sternum and spinous process markers on the sagittal plane and the line connecting the origin of the X-ray system of coordinates and the center of the screen. The relationship between the coordinates of each marker and the angles α and β was expressed as follows (Fig. 4).

$$\begin{aligned} \text{Tan}\alpha &= (X_2 - X_1) / |Z_2 - Z_1| \\ \text{Tan}\beta &= (Y_2 - Y_1) / |Z_2 - Z_1| \end{aligned} \tag{Formula 4}$$

Table 1. Trunk movements due to abduction of shoulder

Abduction of Shoulder (degree)	Sagittal plane		Frontal plane		Horizontal plane	
	healthy group	impaired group	healthy group	impaired group	healthy group	impaired group
0	3.2±1.9	2.6±2.0	0.7±0.8	1.5±0.9	3.0±2.4	3.6±1.0
30	3.5±2.1	3.5±2.6	1.0±1.1	1.8±1.9	2.8±2.4	3.9±2.4
60	3.1±1.8	3.0±2.1	1.7±1.4	3.5±4.1	2.3±2.5	4.3±2.2
90	3.6±2.0	3.0±2.5	1.7±1.4	5.0±2.4	2.3±2.4	8.8±3.3*
120	6.0±3.8		2.8±2.1		2.8±2.7	
150	8.6±3.9		1.8±1.2		2.3±2.3	
180	12.2±4.4		1.3±1.7		4.0±2.6	

(degree, Mean±SD, * p<0.05)

In the results of the healthy group and the impaired group, the difference in the trunk rotation angle at 90 degrees of shoulder abduction was statistically significant (p<0.05), but the others were not significant.

Angles α and β were calculated from formula 4 using the inverse tangent function.

The angle change (γ) in the frontal plane was measured as the angular difference between the horizontal line on the screen and the transverse axis of the sternum marker.

Statistical analysis software R was used to compare the healthy group and the impaired group, and the Mann-Whitney U test was used, and the significance level was set to p<0.05.

Results

Trunk movements due to abduction of shoulder are shown in Table 1.

Voluntary shoulder abduction up to 180° was observed in the healthy group, while in the impaired group, the maximum voluntary abduction angle was 90° in 3 patients and 75° in 1 patient.

The angle of anteroposterior trunk flexion in the healthy group remained $\leq 5^\circ$ up to 90° of shoulder abduction, but increased beyond 90° of shoulder abduction. No significant changes in the trunk anteroposterior flexion angle were observed regardless of the shoulder abduction angle in the impaired group. The angle of lateral trunk flexion remained $\leq 5^\circ$ in both the healthy and impaired groups; however, in the impaired group, the greater the angle of shoulder abduction, the greater the difference from the healthy group. The trunk rotation angle did not change significantly in the healthy group regardless of the shoulder abduction angle; however, the trunk rotation tended to increase with shoulder joint abduction in the impaired group.

In the results of the healthy group and the impaired group, the difference in the trunk rotation angle at 90 degrees of shoulder abduction was statistically significant (p<0.05), but the others were not significant.

Discussion

Upper limb function is involved in almost all activities and is important in ADL. Many shoulder movements require an adequate range of motion, and shoulder abduction of approximately 100° is necessary for ADL such as washing the body and combing hair. Thus, it is clinically important to restore shoulder abduction $> 100^\circ$.

The shoulder joint is moved using combined efforts from the anatomic glenohumeral joint consisting of the humerus and scapula and a functional scapulothoracic joint consisting of the scapula

and thorax. If the shoulder joint is damaged, such as with rotator cuff injuries or adhesive capsulitis, the movement of the scapula associated with the movement of the upper limb is said to be different from that in healthy individuals⁷. If shoulder joint mobility is reduced, the scapula compensates and, if this is insufficient, compensatory trunk movements may occur. In addition, from the perspective of rehabilitation medicine, it is necessary to secure the maximum range of motion of each joint in order to enable ADL; however, if there are limitations, compensatory movements should also be utilized. On the other hand, excessive compensatory movements may reduce the function of the original joint. Therefore, it is clinically important to analyze and evaluate the kinematics of compensatory movements.

To date, various kinematic analyses have been developed for the objective evaluation of shoulder joint movement. In general, the analysis is performed using a goniometer and a ruler on radiographs^{3,4}); however, because the analysis is performed using projection images, three-dimensional analyses are difficult. To solve this issue, an analysis using radiographs that were simultaneously taken from the front and a 90° angle has been reported; however, a special shooting table was required⁵. Kinematics analyses using CT/MR images have also been reported; however, radiation exposure and limitation of the position of the limb being imaged pose issues.

Recently, there have been several reports of kinematics analyses using 2D-3D registration. This is a method to estimate the position and posture based on the moving distance of the coordinates by setting spatial coordinates in 3D models obtained from CT or MR imaging and matching these with 2D radiographs^{1,2}), and this enables measurement, including movements over time, in a relatively noninvasive manner.

However, in all reports, the patient position during radiography was not strictly defined, and the analyses were performed assuming that the posture of participants during imaging was constant. Therefore, in the present study, the effects of compensatory trunk movements on shoulder joint kinematics during radiography were evaluated.

In the healthy group, trunk retroflexion $>5^\circ$ was observed after shoulder abduction of at least 120° . In general, extension of the vertebral column, that is, retroflexion of the trunk, is required in the late phase of shoulder abduction, and the mechanism is considered to be the contraction of the lower trapezius fibers, which are involved in the retroflexion of the trunk, moving the scapula downward, leading to the extension of the vertebral column and retroflexion of the trunk. The trunk retroflexion in the healthy group in this study was considered to represent the aforementioned physiological movements.

In the impaired group, lateral flexion of the trunk to the contralateral side and rotation of the trunk to the ipsilateral side exceeded 5° in the final range of shoulder abduction. In healthy shoulder joints, the scapular glenoid fossa is smaller than the humeral head, resulting in greater mobility; however, the fit is shallow and stability is poor. The humeral head is covered by four rotator cuff muscles and stabilized by pressing against the glenoid fossa. In this manner, the deltoid muscle, the main movement muscle, works effectively in coordination with the rotator cuff muscles, causing the glenohumeral joint to abduct. RSA is indicated for surgery in patients with rotator cuff tear arthropathy and wide ruptures of the rotator cuff that cannot be repaired temporarily in the elderly presenting with pseudoparalysis where it is difficult for the patients to raise their arm by themselves^{6,7}). Therefore, in the impaired group, the deltoid muscle did not work effectively and mobility decreased due to instability of the shoulder joint caused by the decreased function of the

rotator cuff muscles. Walker et al reported^{8,9)} that in rotator cuff tear, shoulders with reduced rotator cuff function, and post-RSA shoulders, the shoulder joint mobility decreases, and upward rotation of the scapula increases during shoulder abduction. Trunk rotation in the impaired group is thought to compensate for the upward rotation of the scapula due to the deltoid muscles not working effectively, which in turn is caused by the decreased function of the rotator cuff muscles, resulting in decreased shoulder joint mobility. However, securing sufficient mobility is insufficient, and additional lateral bending of the trunk toward the measured side and contralateral side should be considered to compensate for shoulder abduction.

In addition, humeral external rotation is required for shoulder abduction in the frontal plane in healthy shoulders since the humeral head passes through the subacromial space at 90° of shoulder abduction, while humeral external rotation is not required for shoulder abduction in the scapular plane (horizontal adduction of approximately 30° from the frontal plane), and abduction is easier to perform than that in the frontal plane. In the impaired group, the function of the rotator cuff muscles was reduced, and abduction in the scapular plane, which is more prone to abduction, was considered to be attempted during shoulder abduction. However, since shoulder abduction in the frontal plane was indicated at the time of radiographic evaluation, participants were considered to be performing apparent shoulder abduction in the frontal plane by performing compensatory movements of rotating the trunk ipsilateral to the measured side and aligning the scapular plane with the horizontal plane.

In the healthy group, physiological movements of trunk retroflexion were observed after shoulder abduction of at least 120°, and in the impaired group, compensatory trunk movements were observed in the final range of shoulder abduction. When evaluating the shoulder joint on radiographs, attention must be paid to the physiological movement of trunk retroflexion in the sagittal plane even in healthy individuals. In addition, attention must also be paid to compensatory trunk movements such as trunk lateral flexion and rotation in the frontal and horizontal planes in patients after RSA surgery with reduced rotator cuff function.

Limitations of this study include the small sample size and healthy individuals being younger than the impaired group. Since thoracic vertebral kyphosis and shoulder girdle function change and scapular and humeral kinetics differ in the young and the elderly^{10,11)}, there is a need to perform evaluations in groups with wider age ranges. Furthermore, there is a need to clarify the relationship with compensatory trunk movements in more detail by conducting studies that include assessments of muscle strength and the range of motion of other joints.

Simultaneous evaluation of the shoulder joint and compensatory trunk movements may provide rehabilitation programs to improve activities of daily living. Unrestricted free shoulder abduction may result in even greater trunk compensatory movements, and when performing clinical rehabilitation, it is necessary to pay attention to trunk movement and flexibility in addition to the glenohumeral joint and scapulothoracic joint. In the future, we hope to evaluate how compensatory trunk movements affect actual ADL and to develop more effective rehabilitation programs.

Acknowledgements

All authors have no COI to declare regarding the present study.

References

1. Yamazaki N, Watanabe T, Sato Y, et al. CAD based on 2D-3D registration and visualization. Medical Imaging

- Technology 2006;24:94-100.
2. Mahfouz MR, Hoff WA, Komistek RD, et al. A robust method for registration of three-dimensional knee implant models to two-dimensional fluoroscopy images. *IEEE Trans Med Imaging* 2003;22:1561-1574.
 3. Inman VT, Saunders JB, Abbott LC. Observations of the function of the shoulder joint. 1994. *Clin Orthop Relat Res* 1996;(330):3-12.
 4. Freedman L, Munro RR. Abduction of the arm in the scapular plane: scapular and glenohumeral movements. A roentgenographic study. *J Bone J Surg Am* 1966;48:1503-1510.
 5. Bey MJ, Zauel R, Brock SK, et al. Validation of a new model-based tracking technique for measuring three-dimensional, in vivo glenohumeral joint kinematics. *J Biomech Eng* 2006;128:604-609.
 6. Boudreau S, Boudreau ED, Higgins LD, et al. Rehabilitation following reverse total shoulder arthroplasty. *J Orthop Sports Phys Ther* 2007;37:734-743.
 7. Hatzidakis AM, Norris TR, Boileau P. Reverse shoulder arthroplasty indications, technique, and results. *Techniques in Shoulder and Elbow Surgery* 2005;6:135-149.
 8. Mell AG, LaScalza S, Guffey P, et al. Effect of rotator cuff pathology on shoulder rhythm. *J Shoulder Elbow Surg* 2005;14:58S-64S.
 9. Walker D, Matsuki K, Struk AM, et al. Scapulohumeral rhythm in shoulders with reverse shoulder arthroplasty. *J Shoulder Elbow Surg* 2015;24:1129-1134.
 10. Dayanidhi S, Orlin M, Kozin S, et al. Scapular kinematics during humeral elevation in adults and children. *Clin Biomech (Bristol, Avon)* 2005;20:600-606.
 11. Endo K, Yukata K, Yasui N. Influence of age on scapulo-thoracic orientation. *Clin Biomech (Bristol, Avon)* 2004;19:1009-1013.

Orbital Venous Malformation with Obscure Clinical Symptoms Diagnosed by Contrast-enhanced Magnetic Resonance Imaging in a Different Body Position

AKIKA KYO¹⁾, YUSAKU YOSHIDA²⁾, MIZUKI TAGAMI¹⁾, MASAO HAMURO³⁾, and SHIGERU HONDA¹⁾

*Department of Ophthalmology and Visual Sciences¹⁾,
Osaka City University Graduate School of Medicine; and
Departments of Ophthalmology²⁾ and Radiology³⁾, Izumiotsu Municipal Hospital*

Abstract

Orbital venous malformations are the most common type of orbital vascular anomaly. The main initial complaints are presence of a mass, proptosis, globe displacement, or hemorrhage. Since the subjective symptoms of this condition usually become noticeable only after the mass has increased in size, small malformations often remain undetected. Imaging modalities such as computed tomography, magnetic resonance imaging, magnetic resonance angiography, and endovascular contrast are commonly used for diagnosis, but are not always successful.

In the present manuscript, we report a case of a 54-year-old woman who presented with acute, severe eye pain and swelling. Only slight subcutaneous hemorrhage was present, and no exophthalmos or eyelid swelling was identified. Precontrast computed tomography and precontrast magnetic resonance imaging were unable to provide a definitive diagnosis. Notably, the patient complained that symptoms worsened when she changed body positions. Bearing this in mind, orbital venous malformation was eventually diagnosed by changing her body position during contrast-enhanced magnetic resonance imaging. Cases of orbital venous malformations without obvious clinical symptoms may exist and magnetic resonance imaging with different body positions could offer a more definitive diagnosis.

Key Words: Imaging; Orbit; Vascular malformation

Introduction

Orbital venous malformation (OVM) is the most common type of venous malformation in the orbit. The main symptoms of OVMs are presence of a mass, proptosis, globe displacement, edema, and hemorrhage around the eyelids, and deep orbital pain.

In addition, distensible OVM demonstrates as an initial small nidus with filling in the pre-Valsalva arterial phase, and progressive filling and expansion in the subsequent Valsalva venous phase. However, such cases usually show obvious clinical symptoms such as visual loss, proptosis, or

Received May 10, 2021; accepted August 27, 2021.

Correspondence to: Akika Kyo, MD.

Department of Ophthalmology and Visual Sciences, Osaka City University Graduate School of Medicine,
1-4-3 Asahimachi, Abeno-ku, Osaka 545-8585, Japan
Tel: +81-6-6645-3867; Fax: +81-6-6645-3873
E-mail: m2071526@med.osaka-cu.ac.jp

spontaneous hemorrhage. As subjective symptoms usually become noticeable when the mass increases in size, small malformations often pass undetected or cause few symptoms.

We report herein a case of OVM that caused few clinical symptoms and could not be diagnosed on precontrast computed tomography (CT) or precontrast magnetic resonance imaging (MRI), but was eventually diagnosed by contrast-enhanced MRI with the patient in a different body position.

Case Report

A 54-year-old woman presented at the emergency room of another hospital with left eyelid pain, left eyelid swelling and nausea. She had previously noticed discomfort around the left eye when lying face down. Results of cranial CT were unremarkable, and as blood tests revealed a slightly elevated white blood cell count, a cephem antibiotic was prescribed. The patient was examined in our department the following day for further ophthalmological investigations. Best-corrected visual acuity was 0.9 on the right and 1.0 on the left, with no other intraocular abnormalities. The bilateral eye movements were also normal, and no exophthalmos was identified. Mild subcutaneous hemorrhage of the left eyelid was present, but left eyelid swelling had improved (Fig. 1). No other objective signs were present. Because the symptoms had improved with antibiotic treatment, orbital cellulitis was initially suspected. MRI revealed a lesion in the extraconal medial rectus oculi muscle and ethmoid sinus wall within the left orbit, appearing hypointense on T1-weighted image and hyperintense on T2-weighted and short T1 inversion recovery (STIR) image (Figs. 2A-2C). Sinusitis was also present in the ethmoid sinus (Fig. 2D). These observations were believed to represent sinusitis-induced orbital cellulitis, and antibiotic treatment was continued.

Two weeks later, the patient complained of left recurrent eye pain that was aggravated when looking downwards. Precontrast MRI and magnetic resonance angiography (MRA) carried out that day showed that the lesion had increased somewhat in size since the previous scans (Fig. 3). The lesion appeared lobulated with an ill-defined edge, but no abnormal vessels suggestive of arteriovenous malformation or arteriovenous fistula were visualized on MRA. The subcutaneous hyperintense signal disappeared within the left orbit, indicating that the subcutaneous hemorrhage was absorbed. A radiologist suggested the possibility of varix or hemangioma, but as the patient did not complain of left eyelid swelling, left eye pain, or other subjective symptoms at that time, watchful waiting was continued.

One month later, the left eye pain recurred. Contrast-enhanced MRI was considered to be required for differential diagnosis, and was therefore performed. The size and shape of the lesion were unchanged from the previous scans (Fig. 4A). In dynamic contrast-enhanced MRI, the lesion started to exhibit contrast enhancement slowly after the sinus venosus, becoming enhanced at almost the same time as the superior ophthalmic vein, and showed strong contrast enhancement in the equilibrium phase. The lesion increased in size when the patient was prone (Figs. 4B and 4C). Based on the findings that the lesion had slow blood flow and increased in size with the prone position, and the lack of demonstrable arterial supply to the lesion, OVM was diagnosed.

After that, she repeatedly complained of left orbital pain without other clinical symptoms even if she changed body positions, so she was referred to the department of neurosurgery for surgical treatment. However, angiography did not visualize any vascular inflow into the orbital tumor, and the decision was made to keep the patient under surveillance without treatment.

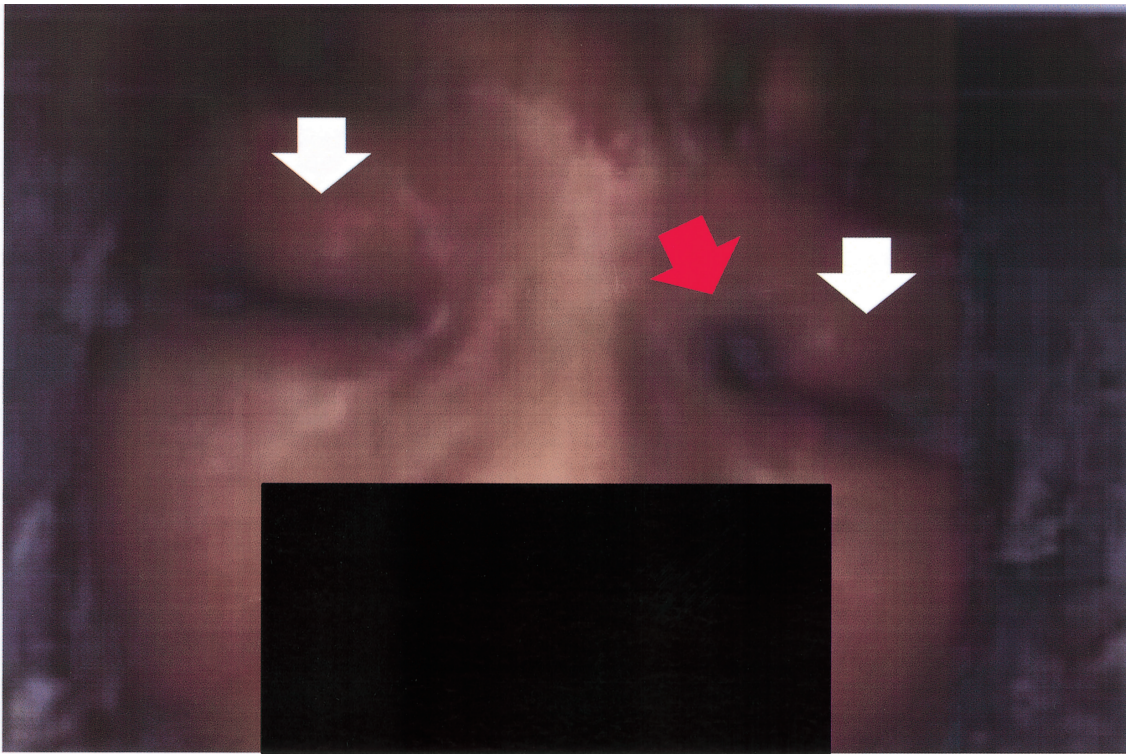


Figure 1. A 54-year-old woman presented with mild subcutaneous hemorrhage of the right eyelid, but eyelid swelling had improved compared to her first visit. No other objective signs were present.

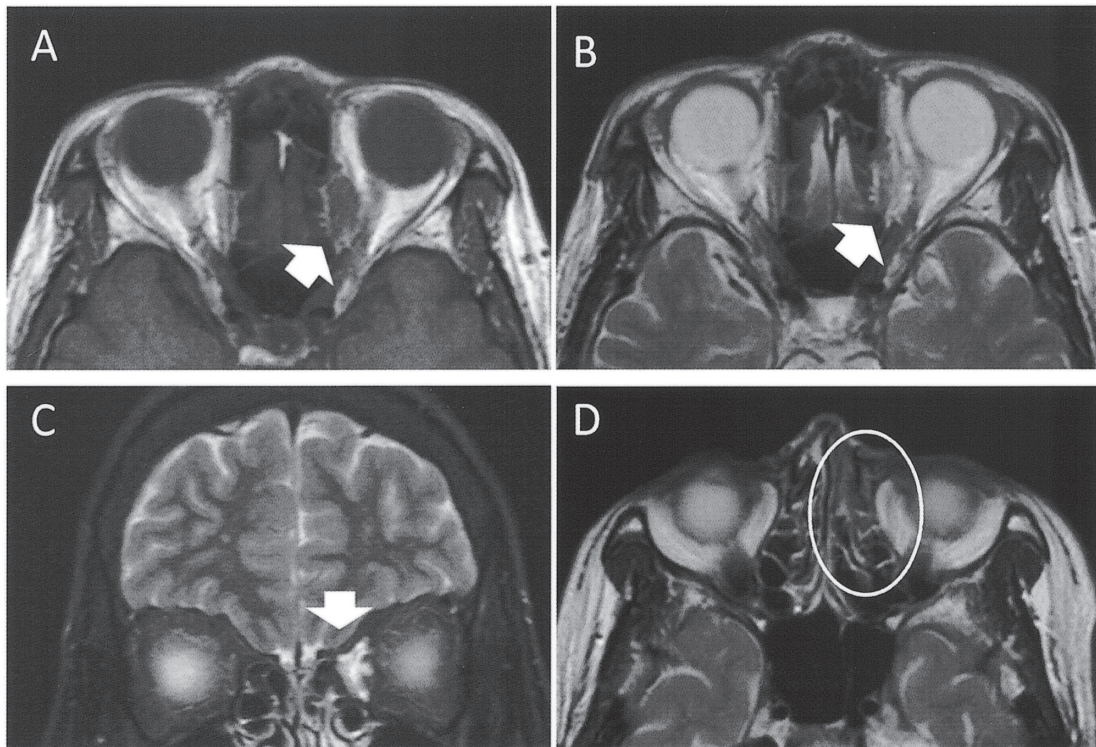


Figure 2. Initial MRI reveals a lesion in the extraconal medial rectus oculi muscle and ethmoid sinus wall within the left orbit (arrows). The lesion appears hypointense on axial T1-weighted image (A) and hyperintense on axial T2-weighted and short T1 inversion recovery (STIR) image (B). The lesion is hyperintense on coronal STIR image (C). Coronal STIR image shows a subcutaneous hyperintensity within the left orbit (D).

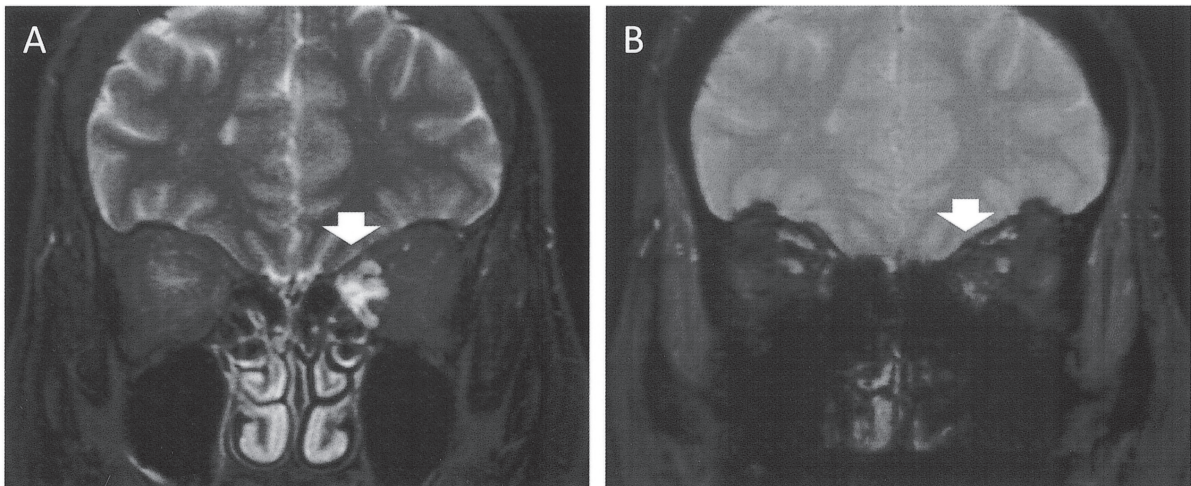


Figure 3. Half a month after her first visit, precontrast MRI shows that the lesion has increased in size since the initial coronal short T1 inversion recovery image (A). The lesion appears to have a lobulated shape with ill-defined edges on T2-weighted image (B).

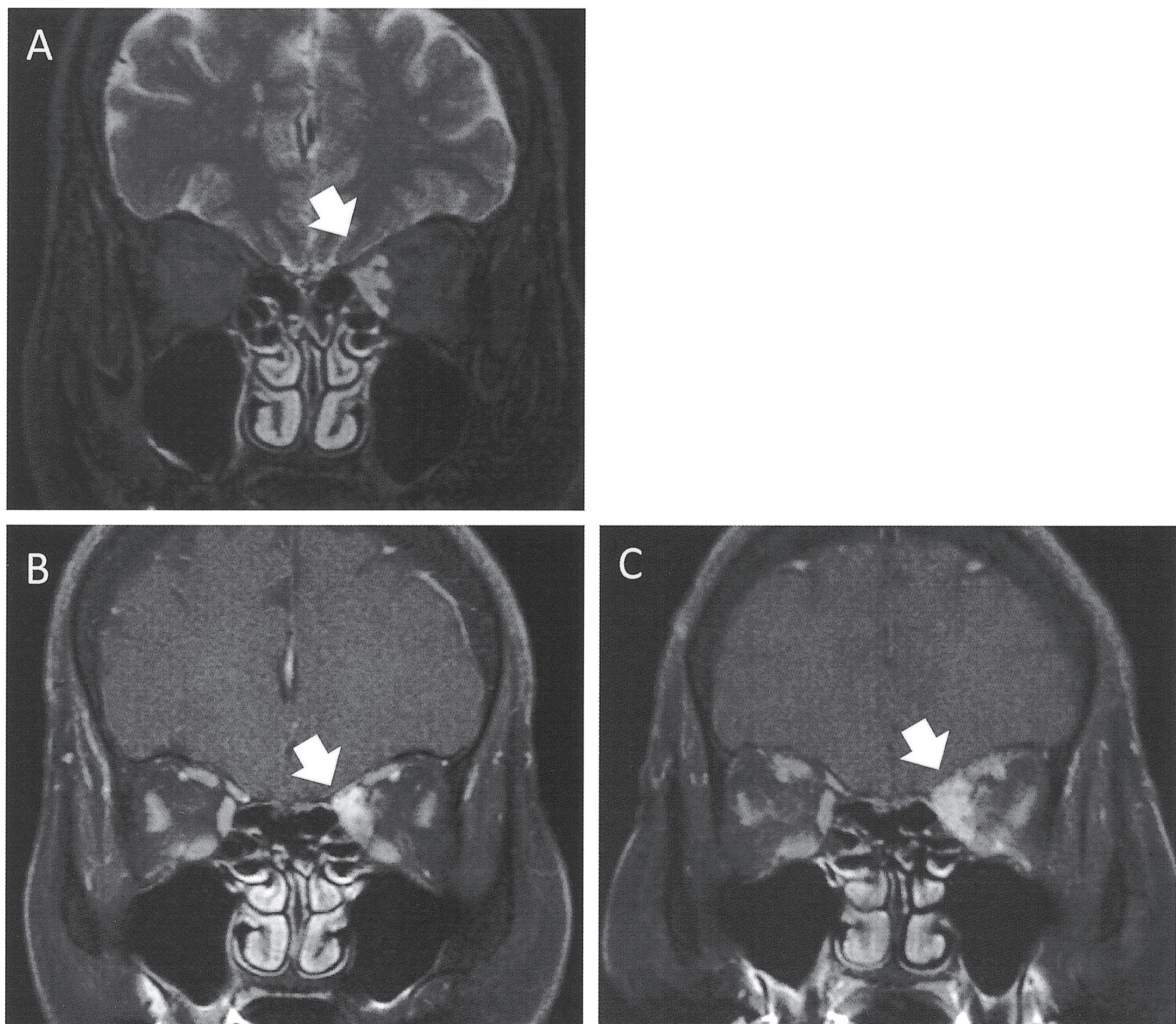


Figure 4. One month after her first visit, the size and shape of the lesion were unchanged from previous scans in the supine position on short T1 inversion recovery image (A). The lesion appears larger in the prone position (C) than in the supine position (B) on coronal contrast-enhanced T1-weighted fat-suppressed MRI.

Discussion

Vascular malformations are subdivided into capillary, venous, lymphatic, arteriovenous, and combined malformations, depending on the dominant vasculature according to the criteria of the International Society for the Study of Vascular Anomalies (ISSVA)¹.

Venous malformations show sluggish blood flow through malformed vessels, and distensible OVM reportedly demonstrates an initial small nidus of filling in the pre-Valsalva arterial phase, with progressive filling and expansion in the subsequent Valsalva venous phase. Nondistensible OVM shows no dilation with the Valsalva maneuver². Usually patients with OVMs complain of the presence of a mass (42%), proptosis (37%), or hemorrhage around the eyelids (15%), then the lesion is detected by performing imaging examinations. CT, MRI, vascular angiography, and other forms of diagnostic imaging are typically used to diagnose OVMs². One study reported that proptosis or eyelid swelling appeared or worsened during the Valsalva maneuver in 52% of cases of orbital arteriovenous malformation³.

In the present case, although main initial complaints were eye pain and eyelid swelling, the only objective finding was slight subcutaneous hemorrhage, and no exophthalmos or eyelid swelling was apparent even during the Valsalva maneuver. However, since pain around the eyelid recurred several times after the hemorrhage was reabsorbed, we carried out some imaging examinations. In dynamic contrast-enhanced MRI, the lesion slowly started to exhibit contrast enhancement after the sinus venosus, becoming enhanced at almost the same time as the superior ophthalmic vein, and showed strong contrast in the equilibrium phase. However, no abnormal arterial inflow into the orbit was identified during angiography. In addition, the lesion enlarged with the patient in a prone position.

This OVM might have been a borderline type between distensible and nondistensible, because the lesion showed negative response to the Valsalva maneuver but positive response to the prone position during imaging. Imposition of a challenge such as a change in body position may thus enable definitive diagnosis in such patients who complain of deep eye pain in the absence of other obvious clinical symptoms.

OVMs that present as intolerable pain, functional defect (usually caused by acute profound hemorrhage), repeated hemorrhage, or chronic cosmetic disfigurement are managed selectively⁴. If intervention is indicated, management options for OVM include sclerotherapy, embolization, detachable coils, laser therapy, or surgical excision^{2,4,5}. In the present case, no obvious OVM was visualized by angiography and the condition was therefore left untreated. The size of OVM may influence whether treatment is indicated.

One issue in this case was that because orbital cellulitis was initially suspected, the possibility of OVM was not raised, and contrast-enhanced imaging or challenges were not used to try to make diagnostic imaging more effective.

Acknowledgements

All authors have no COI to declare regarding the present study.

References

1. International Society for the Study of Vascular Anomalies. ISSVA classification for vascular anomalies. <https://www.issva.org> 2014.
2. Li T, Jia R, Fan X. Classification and treatment of orbital venous malformations: an updated review. *Front*

Med 2019;13:547-555.

3. Wright JE, Sullivan TJ, Garner A, et al. Orbital venous anomalies. *Ophthalmology* 1997;104:905-913.

4. Arat YO, Mawad ME, Boiuk M. Orbital venous malformations: current multidisciplinary treatment approach. *Arch Ophthalmol* 2004;122:1151-1158.

5. Benoiton LA, Chan K, Steiner F, et al. Management of orbital and periorbital venous malformation. *Front Surg* 2017;4:27.

Instructions for Authors

The Osaka City Medical Journal will consider the publication of any original manuscript, review, case report, or short communication. Articles should be in English.

Manuscript submission. Manuscripts should be sent to the Editor, Osaka City Medical Journal, Osaka City Medical Association, Osaka City University Medical School, 1-4-3 Asahimachi, Abeno-ku, Osaka 545-8585, Japan; phone and fax 06-6645-3782; e-mail shiigakukai@med.osaka-cu.ac.jp

The Journal accepts only manuscripts that contain material that has not been and will not be published elsewhere. Duplicate publication of scientific data is not permitted. If closely related papers might be considered to be duplicate publications, the possible duplicate should be submitted with the manuscript and the authors should explain in their covering letter what is original in the submitted paper. Submit three copies of the manuscript (two of which may be photocopies) together with CD-R or DVD-R containing the body text, tables and figures. The manuscript should be prepared by Microsoft Word or its compatible software (doc or docx). Acceptable formats for figures are JPG or TIF. Use only 12-point font size and a standard serif font. Double-space throughout the manuscript and use standard-sized (ISO A4, 212×297 mm) white bond paper. Make margins at least 25 mm wide on all sides. Number pages consecutively starting with the title page and ending with the reference list. Begin each of these sections on a separate page: title page, abstract, text, acknowledgements, references, tables (each one separate), and figure legends. Do not use abbreviations in the title or abstract and limit their use in the text, defining each when it first appears. Manuscripts should meet the requirements outlined below to avoid delay in review and publication. Authors whose native language is not English must seek the assistance of a native English speaker who is familiar with medical sciences. Please attach the certificate from the person(s) who edit the manuscript. Some minor editorial revision of the manuscript will be made when the editorial committee considers it necessary.

Title page. All submissions must include a title page. The full title of the paper, should be concise, specific, and informative, and should contain the message of the paper without being in sentence form. Next, include the full names and academic affiliations of all authors, and indicate the corresponding author, address, phone, fax, and e-mail address. Give a running title (not to exceed 50 characters including spaces), and three to five key words. Last, give the word count for text only, exclusive of title, abstract, references, tables, and figure legends.

Structured abstract. The abstract of 250 words or less should consist of four paragraphs headed **Background, Methods, Results, and Conclusions.**

Text. Full papers about experiments or observations may be divided into sections headed **Introduction, Methods, Results, and Discussion.**

Tables. Each table should be typed on a separate sheet in characters of ordinary size, double-spaced (with at least 6 mm of white space between lines). Each table must have a title and should be assigned an Arabic numeral ('Table 3'). Vertical rules should not be used.

Figures. For black-and-white figures, submit three original glossy prints or laser-quality proofs and three photocopies of each. One transparency and three color prints should be submitted of each color figure. Label the front of figures with the figure number. Indicate on the back of each figure the first author, the first few words of the manuscript title, and the direction of the top of the figure (if needed). Photomicrographs should have scale markers that indicate the magnification. Provide figure legends on a separate page, double-spaced, immediately after the tables. All illustrations and graphs, to be referred to as figures, should be numbered in Arabic numerals ('Fig. 2' etc.). The approximate position of each figure in the text should be indicated in the right margin of the manuscript. Illustrations in full color are accepted for publication if the editors judge that color is necessary, with the cost paid by the author.

References. Reference must be double-spaced and numbered consecutively in the order cited in the text. When listing references, follow the style of the Uniform Requirements (<http://www.icmje.org/>) and abbreviate names of journals according to PubMed (<http://www.ncbi.nlm.nih.gov/sites/netrez>). List all authors up to three; when there are four or more, list the first three and use et al.

Examples of reference style

1. Priori SG, Schwartz PJ, Napolitano C, et al. Risk stratification in the long-QT syndrome. *N Engl J Med* 2003;348:1866-1874.
2. Schwartz PJ, Priori SG, Napolitano C. The long-QT syndrome. In: Zipes DP, Jalife J, editors. *Cardiac electrophysiology: from cell to bedside*. 3rd ed. Philadelphia: W.B. Saunders; 2000. pp. 597-615.

Proofs. One set of proofs together with the original manuscript will be sent to the author, to be carefully checked for any essential changes or printer's errors. The author is requested to return the corrected proofs within 48 h of their receipt.

Short communications and case reports.

1. A short communication should have between 1500 and 2000 words, including the abstract. This word count is equivalent to about four double-spaced manuscript pages.
2. The original and two copies including three sets of figures and tables should be sent to the Editorial Office.

Manuscript submission fee. A nonrefundable fee of 10,000 JPY is due on submission of original manuscripts, case reports, and short communications. A manuscript returned beyond six months of the date of the initial decision will be considered a new submission.

Page charges. A standard publication fee of 100,000 JPY will be applied for each accepted paper. Authors are also required to pay page charge of 10,000 JPY per printed page.
Ex) If your article has 10 pages, the amount of fee is 100,000 JPY + 10 pages × 10,000 JPY = 200,000 JPY.

Reprints. If you were interested in ordering reprints of your article, we accept at least 50 full-color copies. Authors are required to pay page charge of 100 JPY per printed page. Ex) If you request 60 copies for 10-page article, the amount of fee is 100 JPY × 10 pages × 60 copies = 60,000 JPY.

Studies of human subjects. It is the responsibility of the authors to ensure that any clinical investigation they did and report in manuscripts submitted to the Osaka City Medical Journal are in accordance with the Declaration of Helsinki (<http://www.wma.net>).

Animal studies. It is the responsibility of the authors to ensure that their experimental procedures are in compliance with the “Guiding Principles in the Care and Use of Animals” (http://www.the-aps.org/pub_affairs/humane/pa_aps_guiding.htm) published each month in the information for authors of the American Journal of Physiology.

Conflict of Interest (COI) Disclosure.

1. It is the responsibility of the authors to disclose any COI by signing the form.
2. If the authors have no conflicts, please state “All authors have no COI to declare regarding the present study” in the Acknowledgements.

Authors are required to disclose any relationships with company or organization (such as funds, consultancy fee, grant, fee for speaking, stock or shares). At the time of initial submission, the corresponding author is responsible for obtaining conflict of interest information from all authors.

[Revised: June 8, 2021]

COPYRIGHT TRANSFER AND STATEMENT OF ORIGINALITY

We approve the submission of this paper to the Osaka City Medical Association for publication and have taken to ensure the integrity of this work. We confirm that the manuscript is original and does not in whole or part infringe any copyright, violate any right of privacy or other personal or priority right whatever, or falsely designate the source of authorship, and that it has not been published in whole or in part and is not being submitted or considered for publication in whole or in part elsewhere (abstracts excluded).

We agree to transfer copyright the manuscript entitled

to the Osaka City Medical Association upon its acceptance for publication.

Write clearly and signature

(Author: print or type)

(Signature)

(Date)

(Author: print or type)

(Signature)

(Date)

(Author: print or type)

(Signature)

(Date)

(Author: print or type)

(Signature)

(Date)

(Author: print or type)

(Signature)

(Date)

(Author: print or type)

(Signature)

(Date)

(Author: print or type)

(Signature)

(Date)

(Author: print or type)

(Signature)

(Date)

(Author: print or type)

(Signature)

(Date)

(Author: print or type)

(Signature)

(Date)

(Author: print or type)

(Signature)

(Date)

OCMJ for Conflict of Interest (COI) Disclosure Statement

The purpose of this form is to provide readers of your manuscript with information about your other interests that could influence how they receive and understand your work. The form is designed to be completed and stored electronically. Each author should submit this form and is responsible for the accuracy and completeness of the submitted information.

1. 1) Have you accepted from a sponsor or any company or organization (More than 1,000,000 JPY per year from a specific organization) ? (Please circle below)

- (1) Funds ?Yes / No
- (2) Consultancy fee ?Yes / No
- (3) Any grant ?Yes / No
- (4) Fee for speaking ?Yes / No

2) Do you hold any stock or shares related to the manuscript ?

- (1) Directly ?Yes / No
- (2) Indirectly, via family members or relatives ?Yes / No

3) If any of above items are “yes”, please provide detailed information below.

2. If none of the above apply and there is no COI please clearly state “All authors have no COI to declare regarding the present study”.

Manuscript Title:

Name / Signature _____ **Date** _____

Manuscript Identifying Number (if you know it):

Editorial Committee

	Kazuo Ikeda, MD (Chief Editor)	
Yasuhiro Fujiwara, MD	Wakaba Fukushima, MD	Masayuki Hosoi, MD
Koki Inoue, MD	Shoji Kubo, MD	Yukio Miki, MD
Yukio Nishiguchi, MD	Masahiko Ohsawa, MD	Atsushi Shioi, MD
Toshiyuki Sumi, MD	Kishiko Sunami, MD	Daisuke Tsuruta, MD
Junji Uchida, MD		

The volumes and issues published in 1954-2018 were as follows: Vol 1 (one issue), Vols 2-5 (2 issues, each), Vols 6-7 (one issue, each), Vols 8-9 (2 issues, each), Vol 10 (one issue), Vol 11 (2 issues), Vol 12 (one issue), Vol 13 (2 issues), Vols 14-20 (one issue, each), Vol 21 (2 issues), Vol 22 (one issue), Vols 23-65 (2 issues, each), Vol 66 (one issue), Vol 67 (2 issues)

Publisher : Osaka City Medical Association,
Osaka City University Medical School,
1-4-3 Asahimachi, Abeno-ku, Osaka 545-8585, Japan

